Document made available under the Patent Cooperation Treaty (PCT)

International application number: PCT/CA05/000158

International filing date: 09 February 2005 (09.02.2005)

Document type: Certified copy of priority document

Document details: Country/Office: US
Number: 60/542,294
Filing date: 09 February 2004 (09.02.2004)

Date of receipt at the International Bureau: 13 April 2005 (13.04.2005)

Remark: Priority document submitted or transmitted to the International Bureau in compliance with Rule 17.1(a) or (b)

PCT/CA 2005/000
MARCH 2005 14·03·05

PA 1289222

THE UNITED STATES OF AMERICA

TO ALL TO WHOM THESE PRESENTS SHALL COME:

UNITED STATES DEPARTMENT OF COMMERCE

United States Patent and Trademark Office

March 01, 2005

THIS IS TO CERTIFY THAT ANNEXED HERETO IS A TRUE COPY FROM THE RECORDS OF THE UNITED STATES PATENT AND TRADEMARK OFFICE OF THOSE PAPERS OF THE BELOW IDENTIFIED PATENT APPLICATION THAT MET THE REQUIREMENTS TO BE GRANTED A FILING DATE UNDER 35 USC 111.

APPLICATION NUMBER: *60/542,294*
FILING DATE: *February 09, 2004*

By Authority of the
COMMISSIONER OF PATENTS AND TRADEMARKS

M. Sias

M. SIAS
Certifying Officer

File No.: S1680162
TWB/cd

IN THE UNITED STATES PATENT AND TRADEMARK OFFICE

ommissioner of Patents and Trademarks
ashington, D. C. 20231

r:

Transmitted herewith for filing is the provisional patent application of:

ventors: AGNES, George R., BAKHOUM, Samuel F.W. and BOGAN, Michael J.

itle: **SOLUTE NUCLEATION AS A FUNCTION OF THE MASS-TO-CHARGE RATIO OF THE NUCLEATION VESSEL**

Enclosed are:

x] Provisional patent application, including cover sheet and 49 pages of specification;
x] A cheque in the amount of **$160 US** to cover the filing fee

x] The Commissioner is hereby authorized to charge any additional fees which may be required in connection with the filing of this application, or credit over-payment, to Account No. 02-1037. A duplicate copy of this sheet is enclosed.

Respectfully,

By: _____
Thomas W. Bailey
Registration No. 36,411

Date: 6 February, 2004

Oyen Wiggs Green & Mutala
#480 - The Station
601 West Cordova Street
Vancouver, B. C.
Canada V6B 1G1

PROVISIONAL PATENT APPLICATION COVER SHEET

First Inventor: AGNES, George R. Citizenship: Canadian
First Inventor's Address: 2387 Huron Drive
Coquitlam, British Columbia
Canada V3J 6Y7

First Inventor's Residence: Coquitlam, British Columbia, Canada

Second Inventor: BAKHOUM, Samuel F.W. Citizenship: Canadian
c/o Simon Fraser University/Industry Liaison Office
Room 3150 Strand Hall
Burnaby, British Columbia
Canada V5A 1S6

Second Inventor's Residence: Burnaby, British Columbia, Canada

Third Inventor: BOGAN, Michael J. Citizenship: Canadian
Suite 901 - 9521 Cardston Court
Burnaby, British Columbia
Canada V3N 4R9

Third Inventor's Residence: Burnaby, British Columbia, Canada

Title: **SOLUTE NUCLEATION AS A FUNCTION OF THE MASS-TO-CHARGE RATIO OF THE NUCLEATION VESSEL**

Agents: Gerald O.S. Oyen Reg. No. 27,280; Blake R. Wiggs Reg. No. 29,505; Bruce M. Green Reg. No. 30,524; David J. McGruder Reg. No. 32,375; Thomas W. Bailey Reg. No. 36,411; Gavin N. Manning Reg. No. 36,412 and George F. Kondor Reg. No. 40,477; Craig A. Ash Reg. No. 48,228; Hilton W.C. Sue Reg. No. 51,325

Agent's Docket Number: S1680162

Correspondence address:
PLEASE ADDRESS ALL CORRESPONDENCE RESPECTING THIS APPLICATION TO:

THOMAS W. BAILEY (Reg. No. 36,411)
Oyen Wiggs Green & Mutala
480 - The Station, 601 West Cordova Street
Vancouver, British Columbia
CANADA V6B 1G1

Please direct all telephone calls respecting this application to **Thomas W. Bailey** at telephone number (604) 669-3432.

Thomas W. Bailey
Registration No. 36,411

Provisional Patent Application

Inventors: Samuel F. W. Bakhoum, Michael J. Bogan, and George R. Agnes
Department of Chemistry, Simon Fraser University, Burnaby, B.C., V5A 1S6

Solute Nucleation as a Function of the Mass-to-Charge Ratio of the Nucleation Vessel

Table of Contents

Page	Section	Title
2	1.0	Overview and definitions
2	2.0	The invention
3	3.0	Introduction to solute nucleation and crystal growth
4	4.0	Background literature on nucleation and crystal growth in selected media
5	4.1	Study of ion-molecule reactions in the gas phase
5	4.2	Studies of nucleation in condensed phase media that did have net charge
6	4.3	Protein crystallization in levitated droplets
7	5.0	Experimental and results
8	5.1	Nucleation studies of dissolved solids in levitated droplets with net charge
8	5.1.1	Experimental apparatus and general procedure for levitation of droplets with net charge
9	5.1.2	Example of the composition of a starting solution for a nucleation study
9	5.1.3	Results concerning the nucleation of CHCA as a function of the mass-to-charge of the levitated droplet
13	5.2	Measurement of droplet mass and net charge
13	5.2.1	Overview
13	5.2.2	Introduction
14	5.2.3	Experimental
15	5.2.4	Results
18	5.3	Effect of a DC potential on a substrate while a liquid droplet dries to a solid residue
19	6.0	Potential areas of application
20	6.1	Illustration of how this invention could be applied to the growth of crystals of a MALDI matrix within which an analyte compound co-precipitates
20	7.0	Summary
21	8.0	List of tables
25	9.0	List of figures
43	10.0	References

1.0 OVERVIEW AND DEFINITIONS

We have acquired evidence that indicates the magnitude of the net charge, and more specifically the mass-to-charge ratio of a nucleation vessel affects the nucleation of a dissolved solid. The vessel may be a droplet with net charge, though in general, it could be any medium in which there is a net charge. Those droplets were created and levitated in an electrodynamic balance (EDB) at atmospheric pressure in our laboratory using existing technology, and it is within the levitated droplets that we have observed a charge-induced nucleation phenomenon that results in the generation of nuclei of a dissolved solid, versus aggregates, when the mass-to-charge ratio of the nucleation vessel is decreased.[1] This suggests that the mass-to-charge of the nucleation medium affects the magnitude of the barrier for a dissolved solid to nucleate. However, it is important to recognize that our methodology restricted our determination of whether or not nucleation took place only after the levitated droplet residues had been deposited onto a substrate. In droplets in which nucleation did not occur, either solute aggregation or no solute precipitation was observed, rather than nucleation.

These experiments were made possible through the use of our previously disclosed apparatus for droplet generation, levitation, and deposition.[1] In addition, the further development of that technology and our expertise regarding its use, has allowed us to measure the mass-to-charge ratio of levitated droplets in which nucleation did or did not occur.

Definition of terms used in this document:

Starting solution This refers to a solution whose composition is known, and easily replicated. An aliquot of the starting solution was delivered to the droplet-on-demand ink-jet style droplet generator.

Initial Droplet Using the droplet generator loaded with ~2 μL of a starting solution, a quantity of that solution (typically ~ 100 - 400 picoliters) was ejected from the nozzle on the droplet generator and that aliquot formed a droplet, which is referred to as the initial droplet. The initial droplet could be deposited onto a substrate directly, or injected into an EDB and levitated there for a period of time.

Droplet Residue The solvent in all droplets evaporated, and for example, methanol or water solvent evaporated quickly leaving behind a residue of the original droplet. In that residue of the original droplet were the solvents of lower volatility and all non-volatile solutes. The droplet residue could be referred to as a levitated droplet residue, in which case it was suspended in air inside an electrodynamic balance (EDB), or that residue could be deposited onto a substrate remote from the EDB. (Note, Coulomb explosion, a process that causes a droplet with net charge to fragment was avoided in this work by the addition of a compound which had a high surface tension. Glycerol in the starting solution at ~0.5 to 10% by volume was used in the majority of the starting solutions as a surface tension modifier.

Nucleation The solids of α-cyano-4-hydroxycinnamic acid (CHCA) nuclei appear as transparent white solids with sharp edges when viewed using an optical microscope. Sample pictures of CHCA solids in deposited droplet residues taken with a CCD camera mounted on the trinocular head of the optical microscope are shown in Figure 1, but note that these droplet residues had been deposited on a glass slide.

Aggregation Aggregates of CHCA appear as opaque globular solids when viewed through an optical microscope.

Crystals Crystals of CHCA appear as clear solids when viewed using an optical microscope. Crystals of CHCA are grown on nuclei of CHCA, but not on aggregates of CHCA.

2.0 THE INVENTION

This application is concerned with the nucleation of dissolved solids from solution. It has been found that the energy barrier for dissolved solids to nucleate is affected by the mass-to-charge ratio of the nucleation volume. A reduction in the mass-to-charge ratio of the nucleation medium causes the barrier for nucleation to decrease. In nucleation media that are at low mass-to-charge, a large number of small nuclei are observed. In contrast, in nucleation media at relatively higher high mass-to-charge, when solids did form in those levitated droplets, aggregates were observed often, but nuclei were only seldom observed in the residues of those droplets. These observations suggest that nucleation media that have appropriate mass-to-charge promote the formation of nuclei, and possibly catalyze the nucleation. An example of the formation of a large crystal grown in a nucleation medium having a low relative mass-to-charge is provided. Additional experiments were performed in which the mass and net charge of nucleation media (*i.*e. droplets) were measured, and those results illustrate the capability to make droplets whose mass-to-charge ratio can be varied in a controlled manner. We anticipate that this solute induced nucleation phenomenon in vessel whose mass-to-charge ratio is within a certain range is likely to be general for all dissolved solids, ranging from inorganic compounds, to low and high molecular weight organic compounds, including proteins.

3.0 INTRODUCTION TO SOLUTE NUCLEATION AND CRYSTAL GROWTH

The formation of crystals from a solution consisting of one type of solute can be described in terms of the compounds phase diagram in the medium. The medium is defined by its chemical properties (such as concentration of and types of solvents, electrolyte, pH, buffers, impurities, and the solute(s) of interest) and physical properties (such as type of container, temperature, pressure, magnetic fields, electric fields, gravity). Provided the phase diagram is known, or can be established through experiment, crystals of a dissolved solid can in principle, be obtained. For example, the crystallization of inorganic compounds for which phase transitions and phase diagrams can be measured, theories of crystal nucleation and growth can and are applied successfully.**[2-8]**

However, despite the development of solute nucleation and crystallization theory over a period of at least 100 hundred years, the simple fact that the formation of a macroscopic crystal of dimensions >1 μm requires the formation of nanoscopic nuclei is significantly more easy to understand than actually demonstrate. Stated differently, it is believed that nuclei on the scale of only a few nanometers form and disappear rapidly in the nucleation medium (*i.*e. an equilibrium process). A key step is to coax, through adjustment of the chemical and/or physical description of the nucleation medium, those nuclei to grow to a critical size such that they spontaneously grow. The degree of supersaturation of the solute is an important factor, and the solute concentration needed to cause nuclei to form and then grow into crystals is referred to as 'critical supersaturation'. Once the nuclei has formed, that nuclei must reach a critical size that is dependent on each solute, such that the solute will spontaneously precipitate onto the nuclei causing it to grow into a crystal rather than shrinking in size and ultimately disappearing.

In light of this, it is then conceivable to envision why the theories of crystal growth do not necessarily help the experimentalist determine which conditions in the nucleation medium are necessary for nucleation and growth of crystals for compounds that have not previously been crystallized by experiment. Examples of such compounds include a newly isolated natural product or novel synthesized compounds (such as a new pharmaceutical compound or an analogue of it), or known compounds that have not yet yielded to crystallization attempts (such as soluble or integral-membrane proteins). The crystallization of novel pharmaceutical compounds is in fact regarded by

those who synthesize them as an empirical process that one becomes more and more proficient at through experience.

These practical issues for solute crystallization have led to a large number of crystallization strategies that have led to an even larger number of experimental techniques and methods. An exhaustive review of nucleation and crystal growth has not been performed, but a directed review on solute nucleation and crystal growth in the presence of a charged entity has been performed, and that is summarized here. The rationale for such a focussed literature review is that recently made observations in the Agnes laboratory suggests that the number of nuclei formed is a function of the mass-to-charge ratio of the nucleation medium. Consequently, the literature review that follows included search parameters such as nucleation on charged surfaces, charged-induced nucleation, and levitated droplets which are commonly referred to as container-less and wall-less vessels.

We had made prior measurements of the distribution of an organic dye cation (Rhodamine 6G) within NaCl that results when a droplet with net charge is allowed to dry while levitated.[9] From that work, we obtained a measure of the thickness of the surface layer that contains the net charge on a droplet with net charge. That data told us that droplets with net charge should be described as imperfect conducting spheres because the thickness of the surface layer was several micrometers in thickness which is much larger than the expected thickness of an electric double layer. This suggests that the surface volume is quite different in its chemical and physical description than the interior of the droplet with net charge. The charge induced nucleation phenomenon observed to vary with the mass-to-charge of the nucleation vessel may be as a result of the electric field at the interface between the surface and bulk-like interior volumes within these droplets, plus the fact that electrical neutrality is not maintained in these droplets with net charge. The presence of an electric field (ie. increased net charge, so reduced mass-to-charge ratio) appears to influence the magnitude thermodynamic barrier leading to nucleation of a solute. We believe that the electric field causes the alignment of molecular dipoles of the solutes in the droplet, and that effects a reduction in their internal energy.

4.0 BACKGROUND LITERATURE ON NUCLEATION AND CRYSTAL GROWTH IN SELECTED MEDIA

The literature from investigators that have been identified by us as being involved with studies of solute nucleation and crystallization in levitated droplets are summarized below, as is the literature on solute crystallization studies in other environments that are of potential relevance to this application. We have attempted to categorize the literature in this review into sub-groups with the intention of simplifying this diverse set of studies. No attempt was made to review nucleation, the general principles of which can be found textbooks and peer-reviewed journals whose focus is crystal growth and nucleation.

Numerous investigators have studied organic compound nucleation and crystal growth in container-less (or wall-less) sample vessels levitated in a medium (typically air at atmospheric pressure). The rationale for the use of container-less vessels in which to effect nucleation and crystal growth was to provide a more homogeneous environment in which a crystal could be grown because there was no liquid:solid interface at the wall of the nucleation medium (*ie.* such as a plastic or glass vial).

An application of the container-less vessel (*ie.* a levitated droplet) for nucleation of organic compounds which has received considerable attention is for protein crystallization. Again, the absence of an interface at the solution-container wall was believed to be of significance with respect to avoiding the growth of impure crystals or crystal with defects, and particularly so when the nucleation

experiment was performed at low temperature. The types of levitation of containerless nucleation media (otherwise known as levitated droplets) are acoustic, magnetic, electrostatic, optical, and combinations thereof. Most of these types of levitation have been studied with respect to their utility in forming crystals of organic compounds.

4.1 *Study of ion-molecule reactions in the gas phase*

The relevance of this set of literature in this application is that a tremendous quantity of research has been performed on gas-phase ion-molecule reactions. This body of work has clearly shown that ions act as nuclei for the clustering and growth of aggregates. The structure of these clusters could be of relevance with respect to the nanoscopic nuclei that ultimately grow into crystals, and moreover, gas-phase ion-molecule reactions are widely acknowledged as experiments that provide snapshots of ion solvation in the (liquid) condensed phase. Though in these studies the aggregates are themselves isolated in the gas phase, the aggregate itself could or could not be in a solid or liquid form depending on the temperature of the aggregate.

The scope of ion-molecule reactions is enormous, and those studies span atomic ions and molecular ions as the charge center onto which molecules and atoms cluster around.**[10]** This work has now extended into the gas phase acid-base properties of proteins.**[11]** Synthetic diamond crystal growth is described as the formation of a 13-Carbon center using chemical vapor deposition technology to form C^- in the gas phase that then causes nucleation of carbon as diamond, rather than the more thermodynamically stable graphite form.**[12, 13]**

Ion-molecule clustering and nucleation has been observed for decades in the gas phase, yet analogous experiments which involve ions clustering phenomena in the condensed phase of a medium that has net charge have not been performed. A condensed phase medium that has net charge may mimic the net charge on a gas phase ion. However, condensed phase media in which the mass-to-charge ratio of that medium was adjusted has not been demonstrated or reported in the literature as an experimental variable that influences nucleation in the condensed phase. This is significant because in essentially all condensed phase media in which nucleation has been studied, regardless of the abundance of charged species present in such media, those media had an overall net electrical charge of zero (*ie.* the nucleation media were neutral). At the very least, nucleation in the condensed phase in a medium that has net excess charge has not yet been reported in peer-reviewed journals, and that is in our opinion, remarkable.

Recent observations in the Agnes laboratory suggest that the net excess charge in a nucleation medium (*ie.* the 'charge' in the mass-to-charge of a nucleation medium) is an experimentally accessible variable that affects the magnitude of the barrier for nucleation. This possibility is described in section 5.1

4.2 *Studies of nucleation in condensed phase media that did have net charge*

Note, as delineated in section 4.1 above, it is important to differentiate experiments performed in the Agnes group in which the mass-to-charge of the condensed phase medium was adjusted as an experimental variable affecting nucleation versus the studies summarized here in section 4.2. The studies summarized here were focussed on nucleation and were performed in media that had net excess charge (ie. droplets with net excess charge that were levitated in air or vacuum),**[14]** but significantly, the possibility that the net charge (and thus the mass-to-charge ratio) of the nucleation medium could influence nucleation or crystal growth was not mentioned, nor was it demonstrated.

The literature summarized here used the same basic apparatus for droplet levitation as the Agnes group (*ie.* an electrodynamic balance). One of the experimental variables studied for nucleation was the effect of supercooling the nucleation medium,**[15, 16]** and the properties of the droplet-air interface was speculated to be an important consideration for the initiation of nucleation.**[17]** A study of optical levitation of a nucleation medium that was cooled has also been reported.**[18]**

A single manuscript was found in which the title 'An investigation of solute nucleation in levitated solution droplets', actually mentioned nucleation and levitated droplet.[19] That manuscript dealt with the determination of critical supersaturation for the nucleation of NaCl and NH_4SO_4 systems, which is a process believed to be important in tropospheric aerosols. However, there is no mention of variation of the net charge of the nucleation medium, nor the mass-to-charge ratio of the nucleation medium, which was a levitated droplet. As an another example of the literature from the atmospheric community regarding the transition from liquid phase to solid phase in aerosols, the Leisner group has published several reports on the nucleation of atmospherically relevant compounds in levitated droplets.[20, 21] Still others use the electrodynamic balance to study reactions at the particle-air interface (*ie.* heterogeneous reactions),[17, 22-34] and phase transfer and freezing processes.[18, 20, 35, 36] The motivation for conducting many of these studies was the hypothesis that reactions at the droplet/particle-air interface are of primary relevance with respect to understanding the science of the troposphere and stratosphere.

Other reports of chemistry in levitated droplets range from simple acid-base reaction in a picoliter vessel,[37] to reactions that were photochemically initiated.[38-42] Optical levitation has also been used to study similar reactions. Cederfelt and co-workers described the charge limit for a droplet in which NaCl could be crystallized in a levitated droplet.[43] Basically, they were interested in determining the maximum net charge that could be contained in a droplet which dried to a solid residue of NaCl without the droplet undergoing a Coulomb explosion. Coulomb explosion is a process by which a droplet with net charge fragments because the repulsive force of its net charge exceeds the attractive force of the droplet, which is a function of the droplet's surface tension and radius.[44-46] There was no mention in the Cederfelt and co-worker manuscript of a change in the nucleation rate or abundance of nucleation sites as a function of net charge (likely because they were nucleating NaCl which is arguably the easiest compound to form crystals of).

In related studies that are of direct relevance to Coulomb explosion, the charge loss from single levitated droplets has been described in a number of manuscripts in recent years.[45-52] The process of a droplet with net charge releasing some of that charge (*ie.* Coulomb explosion) has received considerable attention because of the introduction of Electrospray Mass Spectrometry for the characterization of biomacromolecules by John Fenn.[53-55] Interestingly, a charged cluster, which is a collection of molecules together with one or more ions that is viewed as being an entity intermediate between the gas and condensed phases, can be produced in abundance in an Electrospray.[56-77] The propensity to produce charged clusters in an Electrospray has been recently exploited by Fernandez de la Mora in his experiments that involved studies of neutral molecule clustering around small charged clusters.[78, 79] Again, this is reminiscent of the classic gas-phase ion molecule clustering studies summarized in section 4.1. Protein clusters produced by an Electrospray have also been observed in the gas phase[80-83] and also after their deposition onto a surface.[84]

4.3 *Protein Crystallization in Levitated Droplets*

Though not a defining characteristic of the experimental techniques of this group, many studies have used acoustic levitation to suspend droplets in air in which protein crystallization was studied.[85-87] One of the investigators, Staffan Nilsson, in this group is known by us to be currently active. Nilsson has claimed that his technique is of general utility because his methodology allows for experiments to be designed to learn of the optimal conditions in which nucleation is initiated while, importantly, each one of his experiments consumes only picoliters of sample solution.[88-90] A company in San Diego has also described a similar approach, with respect to the consumption of only picoliters of sample solution per experiment.[91] This company did not utilize levitation, but they were using similar droplet generators (*ie.* ink-jet style droplet-on-demand generators) and that was the foundation for their automation of the experimentation work needed to define optimal conditions for protein crystallization.[91] Of potential interest is the Nilsson group has an article that, as of Dec. 9,

2003, was listed on the articles ASAP webpage of the ACS journal Analytical Chemistry in which the partitioning of a compound between two liquids that were immiscible and contained in an acoustically levitated droplet is described.

Other groups have used a combination of acoustic and electrostatic forces to levitate a droplet, and in some reports, deliberately caused the levitated droplet to rotate slowly in an effort to simulate a space environment (*ie.* the condition of microgravity) while proteins were allowed to crystallize.**[92-98]** Chung and co-workers have described at length how the net elementary charge in their levitated droplets was restricted to the surface of the levitated droplet.[93-95] To them, this was an important feature of their nucleation medium because they felt that a 'homogeneous interior' volume of the droplet, and specifically that its net neutral charge was an important factor in allowing proteins to nucleate, and then grow into crystals. These authors described the volume of liquid surrounding the 'homogeneous interior' as containing the net charge in the droplet. These authors gave the impression that the electric field on the surface of the levitated droplet (due to the net excess charge carried by the droplet) would (or could?) interfere with protein crystallization. We speculate that the mass-to-charge ratio of the droplets levitated using a combination of acoustic and electric forces in the studies by Chung and co-workers were, based on our work discussed in section 5, well above the threshold necessary to observe effects on the nucleation of a solute.

Another set of groups have been using optical trapping and its forces to promote crystal growth, and they can also transfer those crystals to a growth solution (*ie.* seeding).**[99]** Other groups are simply using the intense electric fields of a focused laser beam to induce nucleation.**[100-103]** There is one report of the use of laser ablation for crystal growth, and that report was applied to diamond growth.**[104]**

Of possible relevance to the crystallization of proteins are the types of interactions between proteins and various substrates. Theories of protein crystal growth are now emerging in which a protein, charged because its functional groups are protonated or deprotonated (*ie.* $-NH_2$ OR -COOH respectively) at the condition of the nucleation medium being studied, require the co-precipitation of counter-ions in the growing crystal to maintain near-zero, or zero, electrical neutrality in the crystal.**[105]** The electrical considerations of protein crystal growth have also begun to be explored in both experiment and theory.**[106-109]** Electrostatic forces in crystal alignment have been characterized for liquid crystals**[110]** and micro-ion disposition,**[111]** These findings could be of relevance to protein crystal growth.

A well-known phenomenon that deserves mention here is that the interaction of intact cells with substrates has been studied in detail. Most studies have concluded that electrostatic interactions, at least for cell-substrate interactions, are important.**[112-117]** The sorption of organic compounds onto inorganic compounds has also be studied extensively,**[118, 119]** and the study of the range of chemical reactions catalyzed on such surfaces remains an active area of research.**[120-130]** A related discipline is biomineralization, which involves the use of organic compounds such as proteins to promote or catalyze the formation of solids of inorganic compounds.

5.0 EXPERIMENTAL AND RESULTS

The following description of experimental details and experimental results is presented in two parts. The first part (section 5.1) describes an observation regarding the nucleation of an organic compound in a levitated droplet, and the reproduction of that observation that led to the realization that the mass-to-charge ratio of the nucleation medium, a levitated droplet in this work, influences the nucleation of a solute. The second part (section 5.2) describes the measurements of droplet mass and net charge, and the filtering of droplets with net charge (*ie.* the nucleation vessels in the work described in section 5.1) as a function of their mass-to-charge ratio. Section 5.2 has its own experimental and

results sections because that work was performed independently of the work from section 5.1. The third part (section 5.3) describes the effect of allowing a droplet dispensed from a micropipette to be deposited on to a biased plate.

5.1 Nucleation Studies of dissolved solids in levitated droplets with net charge

5.1.1 *Experimental Apparatus and General Procedure for Levitation of Droplets with Net Charge*

The platform for droplet levitation used in the Agnes group has been described in the literature and in an earlier published patent application (Figure 2).**[1, 131]**

The experiment begins with the preparation of a starting solution that is loaded into a commercially available droplet generator (Microfab, Plano, TX, USA). This droplet generator is an ink-jet style, droplet-on-demand generator that requires as little as 2 μL of starting solution to function. An induction electrode placed near the orifice of the droplet generator, and the DC potential applied to that electrode, is used in conjunction with the time-dependent waveform applied to the droplet generator to make a droplet that has mass and net charge. The induction electrode was made of copper, and it was disk shaped with a 4 mm diameter hole cut in its center. The droplet generator nozzle was centered over the hole in the induction electrode and the vertical separation between the nozzle and the induction electrode was ~2 mm. Unless otherwise stated, the induction potential was + or - 50 V relative to ground potential.

Note, the droplet generator is analogous to an ink-jet printer head, and the details of how it was used in this work are as follows. Each droplet was generated by applying a time-dependent waveform to an annular shaped piezoelectric crystal bonded to the outside of the glass capillary of the droplet generator. The size of the piezoelectric crystal change and the time dependence of that crystal size change effected by the amplitude and temporal characteristics of the AC waveform respectively, create a pressure wave inside the glass capillary of the droplet generator. In turn, that pressure wave forces a volume of liquid out of the nozzle of the droplet generator. While that volume of liquid is emerging from the nozzle, it takes on the form of a jet, and the DC potential applied to the induction electrode induces a net charge onto that jet of liquid such that when the momentum imparted into the jet causes that jet to separate from the nozzle and the jet collapses into a droplet, that droplet has a net charge. The droplet generator is positioned such that each droplet flies into the center of an electrodynamic balance (EDB), where it can be trapped and levitated provided the electric field and the droplet's mass-to-charge are appropriate.

Immediately upon formation of the droplet, the solvents in that droplet begin to evaporate. One or more of the solvents in the droplet are of low viscosity and high vapor pressure. These solvents rapidly evaporate, typically within seconds after formation of the droplet. This solvent evaporation is occurring while the droplet flies to the EDB and continues while it is levitated in the EDB. The starting solutions used in this work incorporated glycerol at a few percent by volume. Glycerol is a solvent of high viscosity and low vapor pressure to avoid Coulomb explosion and enable droplet lifetimes on the order of hours (though the droplet were often levitated for only a few minutes). The physical and chemical description of the levitated droplet after the rapid evaporation of its volatile solvents is a function of the starting solution composition, the conditions used for droplet generation, whether or not Coulomb explosion occurred, and the environmental conditions such as temperature and humidity in the chamber in which levitation was being performed. We will refer to the levitated droplet at this time in the experiment as a residue, in the sense that its composition, though known, is at this stage quite different than the composition of the starting solution.

Following a period of levitation which can range from a few milliseconds to hours, the droplet residue is deposited onto a substrate remote from the EDB by adjustment of the electric field in the EDB. At this point in an experiment, we are able to characterize the composition of the deposited droplet residue for solids using instrumental techniques. This entire procedure which has been

described in serial (*ie.* creation, levitation, and deposition of a droplet) can be made parallel with respect to a sequential and rapid injection of multiple droplets into the EDB, levitating all of them for the duration of a pre-determined levitation period and then causing their sequential deposition. Furthermore, multiple droplet residues levitated in the EDB can be co-deposited onto a single location on a target, or deposited individually, wherein each droplet could be caused to deposit at a different location on the target to form an array of deposited droplet residues.

5.1.2 *Example of the Composition of a Starting Solution for a Nucleation Study*

The starting solution, defined in this document as a solution loaded into the droplet generator, was typically prepared by mixing several volumes of different stock solutions together. Stock solutions were used because one or more of the solutes required dissolution in a particular solvent.

An example of a starting solution with a total volume of 400 µl was prepared by the addition of;
i) 60 µL of a solution containing 20 % glycerol to distilled deionized water by volume
ii) 40 µL of acetone
iii) 40 µL of a solution saturated in α-cyano-4-hydroxycinnamic acid (CHCA) in 50:50 v:v acetonitrile:0.1% TFA in distilled deionized water
iv) 180 µL of acetonitrile
v) 80 µL of distilled deionized water

Another example of a starting solution that contained a different volume of the saturated solution of CHCA was prepared as follows;
i) 60 µL of a solution containing 20 % glycerol to distilled deionized water by volume
ii) 40 µL of acetone
iii) [40 + (x)] µL of a solution saturated in α-cyano-4-hydroxycinnamic acid (CHCA) in 50:50 v:v acetonitrile:0.1% TFA in distilled deionized water
iv) [180 - (0.5 x)] µL of acetonitrile
v) [80 - (0.5 x)] µL of distilled deionized water

5.1.3 *Results concerning the nucleation of CHCA as a function of the mass-to-charge of the levitated droplet*

Example 1

• The number and type of solids in the residues of levitated droplets that had been produced using a positive induction potential (*i.*e. the droplets had net negative charge) has been observed to vary with the magnitude of the DC potential applied to the induction electrode. The results of this experiment in which the only variable was the DC potential applied to the induction electrode are presented in Table 1. (Because this was one of the first reproducible observations of dissolved solids forming in levitated droplet residues as a function of the levitated droplet's mass-to-charge ratio, we had not yet introduced segregation of aggregates versus crystals, nor the size of the solids in the data set in Table 1. This data set refers to the CHCA that had precipitated simply as solids.)

A single waveform was used to generate the droplets produced in this work, and thus the nominal mass of each of the droplets in this work was unchanged within experimental error. Thus the change in the induction potential caused a change in the droplet mass-to-charge ratio.

The composition of the starting solution, total volume = 200 µL, was: i) 30 µL of a solution containing 20 % glycerol to distilled deionized water by volume, ii) 50 µL of a solution saturated in α-

cyano-4-hydroxycinnamic acid (CHCA) in 50:50 v:v acetonitrile:0.1% TFA in distilled deionized water, iii) 120 μL of distilled deionized water

The data in Table 1 indicate that there was an increase in the number of solids present in the residues as a function of the DC potential applied to the induction electrode at the time of formation of the droplets. A higher DC induction potential resulted in a more CHCA solids in the residues of the levitated droplets.

Example 2

• Another nucleation experiment was performed as shown in Figure 3.

In Figure 3, three pictures of sample residues of levitated glycerol droplets are shown. Each of those residues was created from a single starting solution (total volume = 400 μL) that consisted of i) 60 μL of a solution containing 20 % glycerol to distilled deionized water by volume, ii) 40 μL of acetone, iii) 100 μL of a solution saturated in α-cyano-4-hydroxycinnamic acid (CHCA) in 50:50 v:v acetonitrile:0.1% TFA in distilled deionized water, iv) 150 μL of acetonitrile, and v) 50 μL of distilled deionized water. During any one experiment, each droplet was generated from this starting solution using the same waveform applied to the droplet generator. This ensured that within experimental error, the size of all droplets at the instant they were formed were similar. The variable in this experiment was the amplitude of the DC potential applied to the induction electrode. (As a result of levitating droplets whose mass-to-charge ratio was different, the amplitude of the AC waveform applied to the ring electrode and the amplitude of the DC potential applied to the target (*ie.* the deposition plate) were different. There is the possibility that these two factors influence the nucleation of a solid in the levitated droplet, rather than the mass-to-charge of the droplet alone influencing the nucleation of a solid.)

The levitated droplet residues were each deposited after a levitation period of ~3-5 minutes in this experiment. (At this time, we have not repeated these experiments at shorter levitation periods to learn whether the CHCA nucleation occurred before the volatile solvent evaporated, or after.) The pictures clearly show that the nucleation barrier was affected (*ie.* reduced) when the induction potential was raised. The black appearance of globular shaped aggregates are apparent in Figure 3B, whereas sharp edged nuclei that are apparent in Figure 3C are whiter and clearer relative to the solids in Figure 3B.

The number of crystals, and the size of those crystals, from 18 different droplets at each of the induction potentials 100, 150, and 200 V were characterised using an optical microscope (Figure 4). Again, the number of small crystals in the levitated droplets increased with an increase in the induction potential. We believe that the cause of the increased nucleation was the increased net charge per droplet. In the generation of droplets of similar size, an increase in the induction potential lowers the droplet mass-to-charge ratio. The higher net charge in a levitated droplet is believed to cause a reduction on the magnitude of the barrier for nucleation of a dissolved solid in that droplet.

Within the crystal growing community, it is known that the full description of the state of a system should include an electrostatic term, but because crystallisation has almost always performed within a net neutral solution; the electrostatic term is very often simply neglected as an experimental variable. We believe that the use of net charge has not yet been recognised as a controllable variable in the nucleation of a solute in the condensed phase. That statement is not true in the gas phase as numerous ion-molecule reactions have shown how ions act as heterogeneous nuclei onto which neutral compounds condense and cluster around.**[10]** Moreover, the synthetic growth of diamond is because gaseous carbon atoms with a negative charge are formed in a chemical vapour deposition process.**[12, 13]** We believe that our work is the first to demonstrate charge-induced nucleation in the (liquid)

condensed phase for organic compounds. In our laboratory, experiments are on-going to further characterize this charge-induced nucleation phenomenon, including identification of the rate of nucleation, the effect of different polarity of net elementary charge, the range of mass-to-charge and types of organic compounds for which this phenomenon applies, etc.

Example 3

• A nucleation experiment was conducted used a starting solution that was composed of i) 60 μL of a solution containing 20 % glycerol to distilled deionized water by volume, ii) 40 μL of acetone, iii) 100 μL of a solution saturated in α-cyano-4-hydroxycinnamic acid (CHCA) in 50:50 v:v acetonitrile:0.1% TFA in distilled deionized water, iv) 150 μL of acetonitrile, and v) 50 μL of distilled deionized water.

This experiment had two main purposes. First to study the effect of crystallization in the droplets that contain a net positive charge instead of negative, and to have a better understanding of the morphological details of the crystal surface that were apparent using the optical microscope in the Agnes laboratory. From previous results, it was learned that droplets that had been collected on a glass slide which made all the solids appear dark (and resembled coffee beans in appearance) which made it relatively difficult to discern their surface characteristics. Hence, it was decided to collect the droplets on a stainless steel MALDI plate that was chrome plated. The surface of this plate had been machined flat and polished, but because of routine use and abuse the plate actually used was scratched. Crystals within the residues of the droplets deposited from the EDB appeared more shiny and defined under the microscope. However, the small crystals that were observable when the droplets had been deposited onto a glass cover sip, were not observable on the stainless steel plate, possibly because there was not sufficient light available to illuminate the solids sufficiently to allow viewing of the smaller crystals. The crystals observed in the deposited droplet residues, and segregated according to their size are presented in Table 2.

The data presented in Table 2 provide clear evidence that higher relative DC potentials applied to the induction electrode cause the formation of a larger number of crystals relative to when a lower DC potential is used. This experiment was informative to the authors because this was the first time that the number of crystals of CHCA formed were classified according to their size (refer to Figure 4). The large solids, whose size was in the range >3.5 μm in diameter) had an undefined variable shape that appeared to be aggregates, and their surfaces did not shine. The solids whose size was in the range 1.0-3.5 μm in diameter were, in contrast, non-globular in appearance and their surfaces were smoother than the larger solids; these medium size solids appeared more transparent and were likely crystals. The smallest solids observed, <1.0 μm in diameter, are believed to be crystals of CHCA.

Example 4

• The objective of this experiment was to grow a large crystal of CHCA. To this point in our studies, we had shown how the mass-to-charge ratio of the nucleation vessel can be used to preferentially form crystals of CHCA, rather than aggregates. In this example, we studied the potential to grow a single large crystal in a nucleation vessel that was prepared with a mass-to-charge ratio that was in the range in which CHCA nuclei were previously observed to readily form. The levitation period of the nucleation vessel was extended so that the kinetics of crystal growth was not a limiting factor in this experiment.

The starting solution used in this experiment was comprised of; i) 60 μL of a solution containing 20 % glycerol to distilled deionized water by volume, ii) 40 μL of acetone, iii) 40 μL of a

solution saturated in α-cyano-4-hydroxycinnamic acid (CHCA) in 50:50 v:v acetonitrile:0.1% TFA in distilled deionized water, iv) 180 μL of acetonitrile, and v) 80 μL of distilled deionized water.

6 droplets were created with the induction potential set at +80V. +80 V is a relatively low induction potential, and mass-to-charge ratio of these nucleation vessels were relatively high, and thus we did not expect to observe CHCA nuclei in this trial. 3 of these droplets were levitated for 3 minutes before being deposited, and the remaining three were levitated for a total of 12 minutes before they were deposited. No solids (*ie.* no nuclei, aggregates or crystals) were observed in the residues of any of these droplets.

Next, 8 droplets were created at +180 V. +180 V is a relatively high induction potential, so the mass-to-charge ratio of these nucleation vessels was relatively low, and thus we did expect to observe CHCA nuclei in this trial. 4 of these droplets were levitated for 3 minutes, and the remaining 4 droplets were levitated for a total of 12 minutes before they were deposited. No nuclei, aggregates, or crystals were observed within the residues of the 4 droplets levitated for 3 minutes. In one of the droplet residues that had been levitated for 12 minutes, there was a crystal that had a length of 21 μm (Figure 5). In the remaining three droplets that had been levitated for 12 minutes, no solids were observed.

Example 5

• A further experiment was conducted to test the hypothesis that nuclei versus aggregation of CHCA could be unambiguously controlled by setting the mass-to-charge ratio of the nucleation vessel. Thus, the hypothesis was that the barrier for nucleation of crystals versus aggregates can be reduced in nucleation vessels that have a low mass-to-charge ratio.

The starting solution was prepared by the addition of: i) 60 μL of a solution containing 20 % glycerol to distilled deionized water by volume, ii) 40 μL of acetone, iii) 40 μL of a solution saturated in α-cyano-4-hydroxycinnamic acid (CHCA) in 50:50 v:v acetonitrile:0.1% TFA in distilled deionized water, iv) 180 μL of acetonitrile, v) 80 μL of distilled deionized water.

The solids observed in the levitated droplet residues were classified as aggregates or nuclei. The nuclei were further differentiated by size and three size ranges were used.. Large (>3.5 μm in diameter), medium (1.0-3.5 μm in diameter), and small (<1.0 μm in diameter) (Table 3). When solids were formed in these levitated droplets, only aggregates were observed in the droplets that were formed using an induction potential of 100 V (*ie.* relatively high mass-to-charge ratio for the nucleation vessel), but in contrast, only nuclei were observed in the droplets that were formed using an induction potential of 190 V (*ie.* relatively low mass-to-charge ratio for the nucleation vessel).

Example 6

• A further experiment was performed to test the hypothesis that nuclei formed in a nucleation vessel at low relative mass-to-charge could be delivered to another solution, to seed the formation of crystals.

The starting solutions used for this experiment were:

The solution used for droplet generation and subsequent levitation of droplets with net charge was comprised of: i) 60 μL of a solution containing 20 % glycerol to distilled deionized water by volume, ii) 40 μL of acetone, iii) 40 μL of a solution saturated in a-cyano-4-hydroxycinnamic acid (CHCA) in 50:50 v:v acetonitrile:0.1% TFA in distilled deionized water, iv) 180 μL of acetonitrile, and v) 80 μL of distilled deionized water. *The solution pipetted directly onto the glass slide* consisted of a saturated matrix solution of CHCA in 1/1:v/v: ACN/0.1% TFA in distilled deionised H_2O). The volume of this solution pipetted in each case was 50 μL.

To provide a visual reference for CHCA, the solids formed from a solution simply deposited onto a glass cover slip are shown in Figure 6A-6C. CHCA aggregates versus the nuclei are differentiated in these pictures because the former appear globular and dark whereas the latter appear sharp edged and lighter in color. Figure 6A shows some of the largest CHCA crystals formed when a 10 μL aliquot of the starting solution was pipetted onto a glass cover slip and allowed to air dry. Figure 6B is a picture that is representative of the crystals typically observed when an aliquot of the starting solution is pipetted onto a glass cover slip and allowed to dry. Likewise, the picture identified as 6C was taken after a similar aliquot of a starting solution was delivered by pipette onto a glass cover slip that was tilted to cause the solution to spread as a thinner film over a larger surface area of the glass cover slip.

Figure 6D was taken after yet another aliquot of the starting solution was piptetted onto a glass cover slip, but this time, that aliquot of solution was immediately seeded by the deposition of 3 droplets that had been levitated in an EDB. CHCA nuclei were likely present in one or more of those three droplets because they had been created using a relatively high induction potential (x V). Large CHCA crystals are apparent in Figure 6D as a result of this seeding by levitated droplets that contained CHCA nuclei. This experiment can be classified as a two-step crystal design experiment, wherein the 'primary nucleation vessel' could be optimized for the formation of small nuclei of a dissolved solid (*ie.* tuning of the chemical and physical description of a levitated droplet), and 'second nucleation vessel' that is seeded with nuclei could be optimized for crystal growth.

5.2 Measurement of Droplet Mass and Net Charge

5.2.1 *Overview*

The capability to process compounds in levitated droplets with net charge, such as promoting or catalyzing the nucleation of dissolved solids contained within them was introduced in section 5.1 In this section, we describe how droplets with net charge levitated in an EDB can be filtered according to the mass-to-charge ratio of the droplets. This section also delineates our measurements of the actual mass and net charge in individual droplets.

Wall-less sample preparation (WaSP) methodology is built around an electrodynamic balance (EDB), a device that uses AC and DC potentials applied to electrodes to trap charged droplets/particles at atmospheric pressure. Here, the ability of WaSP to preferentially eject specific particles was investigated with a focus on the effect of the mass-to-charge ratio (m/z) of the charged particles. Charged glycerol-based droplet residues on the order of 10^{11} to 10^{12} amu carrying $6x10^5$ to $6x10^6$ net excess charges (polarity: + or -), or $2x10^6$ to $2x10^7$ amu/e, were studied using the current electrode setup. Charged droplets of varied sizes were created and their net excess charge and masses measured using an electrometer and a radiochemical method based on liquid scintillation, respectively. Using these standardized charged glycerol droplets, a series of experiments were performed on pairs of droplets of differing m/z trapped in an EDB that showed droplets were ejected from the EDB in order of highest to lowest m/z. This capability will be useful in studies investigating the chemistry of droplets/particles based on their m/z.

5.2.2 *Introduction*

One of the first, and most celebrated, experiments based on single particles was the Millikan oil drop experiment, performed in 1909.**[132, 133]** By partially suspending single charged oil droplets in a

DC field, Millikan was able to determine the charge of an electron, an experiment for which he was awarded the Nobel prize. Later modification of the experimental apparatus by Wolfgang Paul to include AC fields to trap ions under vacuum led to the development of modern quadrupolar field-based mass spectrometers, and another Nobel prize.[134] The Paul trap technology has since been extended to the trapping of more massive particles by suitable adjustment of the frequencies and amplitudes of the potentials applied to the electrodes of these devices. This resulted in the development of the electrodynamic balance for single aerosol particle characterization. This latter technology has been widely applied to the study of the physical characteristics of single levitated droplets/particles, such as evaporation, charge, and condensation processes.[135-137] Efforts to probe the chemistry occurring in these levitated particles has lead to elegant laser-based probing methods revealing real-time chemical reaction information relevant to atmospheric processes.[30] This sequence of developments demonstrates how important the invention of new technology for manipulation of single particles is to increasing the understanding of their chemistry and physics.

Recent work in our group has focused on the development of new methodology based on the electrodynamic manipulation of charged droplets in an EDB that facilitates a large variety of experiments to be performed. By converting one of the EDB electrodes into a target plate, a procedure for ejecting single droplets and collecting them at known locations (± 5 μm) on the target plate for subsequent analysis was developed[1] (Figure 7). This approach, termed wall-less sample preparation (WaSP), provides access to a diverse set of new experiments based on the electrodynamic manipulation of particles because analysis is not performed during levitation. This enables a myriad of techniques to be used for particle characterization as well as characterization of the impact of the particle on the target onto which it was deposited. Our first efforts involving this technology have focused on its use as a sample preparation device for matrix-assisted laser desorption/ionization (MALDI) because WaSP has the potential to create sample spots small enough to lower the absolute detection limits achieved by this widely applied "soft" ionization source.[131] More recently, we have applied WaSP to probe multi-phase heterogeneous reactions on single aerosol particles and to investigate the partitioning of an organic chromophore within single levitated particles.[9]

Here, using WaSP we investigate the characteristics of the trajectory manipulations of different m/z droplets and demonstrate that droplets are ejected from the EDB in order of highest to lowest m/z. We describe procedures for filtering single particles from populations of up to 50 trapped simultaneously in the EDB as well as the generation of a stream of discrete single particles of a single m/z.

Note that the terms droplet and particle are typically used interchangeably with reference to aerosols levitated in an EDB. The term particle has a broader context including both the solid and liquid aerosols whereas the term droplet is reserved specifically for liquid aerosol particles. Furthermore, the prefix micro- is sometimes added to emphasize the μm-size diameters of the aerosol particles however, for the remainder of the manuscript, we will exclude this prefix because all the particles we work with have μm-sized dimensions.

5.2.3 *Experimental*

Charged Droplet Dispensing All charged droplets studied in this manuscript were prepared using a piezoelectric droplet-on-demand dispenser (Microfab Technologies Ltd., Plano Texas), fitted with a 60 μm diameter orifice.[138] Methanol or aqueous solutions containing 0.8 to 8.0 % glycerol were loaded into the ~ 2 μL internal reservoir of the droplet dispenser using a 10 μL automatic pipette. Droplet formation and charging characteristics are described in detail in the results and discussion section. The charge carried by single droplets was measured by delivering the droplets to a stainless steel plate connected to an electrometer (6517a, Keithley Instruments). A Faraday cage was required to

reduce the background level so that the small charges (femtoCoulomb) carried by each of the droplets could be measured.

Droplet Levitation The EDB used for WaSP has been described in detail earlier and consisted of two copper wire (0.9 mm diameter) rings (2 cm diameter) mounted parallel at a separation distance of 6 mm.[1] The amplitude of the 60 Hz AC potential applied to the ring electrodes (AC_{trap}), in phase, ranged from 500 to 2,700 $V_{0\text{-}P}$. The vertical positions of droplets in the EDB were manipulated by the DC potentials applied to the induction electrode and the MALDI plate. Droplets levitated in the EDB were illuminated via forward scattering by a 4 mW green HeNe laser (Uniphase model 1676, Manteca, California). Images of levitated droplets were collected by focusing a digital camera through a microscope objective to the center of the ring electrodes. Note that to minimize the disturbance of the trajectories of levitated droplets, the droplet generator, the ring electrodes of the EDB, and the target plate were enclosed in a plexiglass chamber to eliminate excessive air flow (Figure 7).

Liquid Scintillation Single droplets were dispensed directly into liquid scintillation vials using time dependent waveforms applied to the piezoceramic droplet dispenser. 2 mL of scintillation cocktail (Amersham Biosciences) was added to the scintillation vial that was then vortexed for 30 seconds. Scintillation is the name given to the detection of fluorescence emission from a compound that was itself excited into an electronic state above the ground state by the absorption of an thermalized electron,and the thermalized electron was the result of quenching a hot electron generated by a nuclear decay event. The detection of the fluorescence emission originating in the scintillation vial enables quantitative measurement of the total number of radionuclides in the scintillation vial

All activity measurements from single droplets and stock solutions were performed using a liquid scintillation counter (LKB Wallac 1217 RackBeta, Fisher Scientific, Montreal, Quebec). Each measurement had an integration time of 10 minutes. Working with ^{32}P requires many safety precautions including the use of plexiglass shielding, a Geiger-Müeller counter, and swipe tests in the working area to monitor for possible spills. Mike Bogan performed these experiments after having received training on the safe handling and disposal of radionuclides.

5.2.4 *Results*

In order to demonstrate the charged droplet filtering capabilities of WaSP we must first establish a reproducible method for creating standard charged droplets of known m/z. Droplets composed of a low volatility solute such as glycerol have long been the vehicle of choice by which studies and modifications of the EDB itself have been performed so we elected to follow this precedent.

To create the glycerol droplets, a solution of 3% glycerol in methanol was loaded into the droplet dispenser's internal reservoir (Figure 2). After applying a potential to the piezoceramic (10-75 V), a droplet was dispensed because the cylindrical piezoceramic reduced its dimensions, constricted the glass sample reservoir and ejected a droplet from the 60 μm orifice at its tip. This commercially available droplet dispensing device was not modified in any way. However, for the dispensed droplets to be levitated in an EDB they must carry net excess charge. An electrode (induction) was positioned 3 mm from the orifice of the droplet dispenser (Figure 8) and by varying the DC potential applied to it (IP_f, the induction potential during droplet formation), the net excess charge carried by the droplets was controlled. The induction electrode had a 2 mm orifice positioned directly in line with the droplet dispenser's orifice so that the droplet was delivered through it towards the EDB.

To measure the net excess charge induced into the single dispensed droplets by the induction electrode, each droplet was captured on a stainless steel plate. Upon impact of the droplet, the charge delivered to the plate was measured using an electrometer with femtoCoulomb (fC) sensitivity. The charge on single droplets prepared with ±10 $V_{0\text{-}P}$ (the minimum required to create a droplet) applied to the piezoceramic in the droplet dispenser delivered too little charge to be measured one at a time so 100

droplets were dispensed at 100 Hz. The total charge delivered was measured and divided by 100 to calculate the average charge carried by single droplets. This experiment was repeated 20 times (2000 droplets) for four different IP_f. Figure 3A shows that the average droplet charge increased linearly as IP_f was increased from 100 to 250 V. Recall that the charge carried by the droplets was actually negative because a positive IP_f was used.

To investigate the reproducibility of single droplet charging, the amplitude applied to the piezoceramic in the droplet dispenser was increased (±30 $V_{0\text{-}P}$) to create larger droplets. This enabled the measurement of the charge carried by single droplets because the droplets were bigger (see mass measurements below) and thus carried more charge. At a fixed IP_f, twenty droplets dispensed at 0.5 Hz and the total charge delivered to the plate was measured after each single droplet impacted with the plate. By repeating this experiment for IP_f set at 9 different values (25, 50, 75, 100, 125, 150, 175, 200, 225 V), droplet charging was deemed reproducible by the linearity of the plot of the total charge delivered as a function of the number of droplets dispensed (Figure 3B, note scale difference relative to Figure 3A). Overall, the data in Figure 9, and similar experiments performed during our studies, show that the charge carried by the droplets was controllable by varying IP_f and the values varied between 5 to 1000 fC per droplet. This corresponds to 3.1×10^4 to 6.3×10^6 net excess elementary charges per droplet.

To calculate the m/z of the droplets created, we must also know the mass of the droplets. A radiochemical method was used to measure the volume of droplets as a function of amplitude applied to the piezoceramic in the droplet dispenser, allowing us to calculate the mass of the droplets. A 100 µL solution of 3.7 MBq ^{32}P labelled orthophosphate in a mixture containing 89.2 % water, 10 % methanol, and 0.8 % glycerol was prepared. By depositing single droplets into liquid scintillation vials and comparing the number of Becquerels measured from them relative to the number measured from a 1.000±0.005 µL aliquot of the ^{32}P in glycerol stock solution, we could determine the volume of the single droplet delivered.

The average activity measured from the single droplets was 0.026±0.001% that measured from the 1.000 µL sample so the average initial droplet volume was $2.6 \times 10^{-4} \pm 1 \times 10^{-5}$ µL or 260 ± 10 pL. The solution loaded into the droplet dispenser to create the droplets contained 0.8 % glycerol by volume so the initial droplets dispensed contained 2 pL of glycerol. When the droplets are levitated in the EDB, volatile solvents rapidly evaporate to leave behind a droplet residue composed of essentially 100 % glycerol. (Corrections to account for the water in the droplet that does vary with the relative humidity of the air in the levitation chamber were made subsequently to these calculations). Therefore, the final droplet volume was ~2 pL. By assuming that the droplet was 100 % glycerol and using the density of glycerol (1.259 g/ml), the mass of the levitated droplets on average was calculated to be 2.5×10^{-9} g. Converting this to atomic mass units (u), the droplets were 1.5×10^{15} u. Recalling that the glycerol droplets carried charges ranging from 5 to 1000 fC, the m/z of the levitated droplets ranged from 9.6×10^8 to 2.0×10^{11} u/e.

Droplets of many different compositions can be prepared using WaSP so it is useful to look at the effect of composition on their m/z. If the percent glycerol in the starting solution was changed to 8 %, the final levitated droplet residue would have a volume of ~21 pL, thereby increasing the mass (and m/z) by 20 times. We have successfully levitated droplets created from solutions containing a percent glycerol by volume of 0.8 to 10 %, creating final levitated droplets of 1×10^{15} to 20×10^{15} u. We have also shown that the charge carried by the droplets can also be varied from 10^4 to 10^6 e. By combining the control of the mass and charge of the glycerol droplets, a wide variety of possible experimental scenarios has been established. Note that these values are many orders of magnitude greater than the typical m/z of ions measured in a quadrupole ion trap mass spectrometer. This characteristic will prove valuable in creating unique applications for this technology in the future.

Now, using the standardized charged glycerol droplets, experiments designed to elucidate whether WaSP could be used to filter the droplets based on their m/z were performed. The general experimental approach was to trap two droplets simultaneously that were created with high m/z and one low m/z relative to each other. By measuring the DC potential applied to the target plate used to eject each droplet, the filtering capabilities of WaSP could be evaluated. An important factor in this experimentation was differentiating between the high and low m/z droplets once trapped. To do this, both high m/z (IP_f = 50 V) and low m/z (IP_f = 100 V) droplets were levitated alone (AC_{trap} = 1600 $V_{0\text{-}P}$) and their respective trajectories were compared. Once trapped, the low m/z droplet immediately adopted a trajectory elongated along the z-axis whereas the high m/z droplet was more focused towards the null point (the center of the EDB). When levitated simultaneously, the high and low m/z droplets adopted trajectories similar to when they were levitated alone so this property was used to identify them (Figure 10A). The images in Figure 10 were collected using a digital camera focussed through a microscope. What was actually photographed was the forward scattering of the green light from the HeNe laser used to illuminate the droplets. When imaged, the droplets did not look like single points because they oscillated at 60 Hz, the frequency of AC_{trap} applied to the ring electrodes (observed at the top and bottom of the images in Figure 10). The shutter speed on the digital camera was not fast enough to capture the droplets in a single spot so the average integrated trajectory of many oscillations of the droplet was captured. This same principle applies to the images in Figure 1 demonstrating the trajectory manipulations of the population of levitated droplets.

To levitate both high and low m/z droplets simultaneously, AC_{trap} was set to 1600 $V_{0\text{-}P}$, a high m/z droplet was levitated, and then a low m/z droplet was injected in to the EDB. Attempts to reverse the order of injection resulted in failure to capture the high m/z droplet. When AC_{trap} was decreased to 1000 $V_{0\text{-}P}$, the trajectory of the low m/z droplet became focused towards the null point, whereas the trajectory of the high m/z droplet moved closer to the induction electrode (Figure 10B). Next, the DC potential applied to the induction electrode was changed to 100 V. The target plate potential was slowly increased until a single droplet was ejected from the EDB and deposited on the target plate (this value was designated the deposition potential, DP). In all iterations of the experiment the high m/z droplet was deposited first. The lower m/z droplet was deposited when the potential applied to the target plate was further increased. This procedure was repeated for droplets created at IP_f = 50 V and IP_f = 150 V, although in this variation of the experiment a larger AC_{trap} (2150 $V_{0\text{-}P}$) was required to trap the two droplets.

Table 4 summarizes the DP measured for each droplet in a series of droplet pairs whose relative m/z varied. Each value in the table is the average of the values measured for five separate pairs of droplets and the errors indicate the magnitude of one standard deviation. Pairs of droplets created at identical IP_f (identical m/z) were ejected from the EDB at the same DP, within experimental error. Notice, however, that the second droplet deposited always required a slightly higher average DP. With droplets created at different IP_f (different m/z), the droplet with the highest m/z was always deposited first. A higher AC_{trap} was required to trap the lower m/z droplets so the DP of a droplet that was created with IP_f = 50 V and trapped with the droplet created with IP_f = 100 V was lower than when it was trapped with a droplet created with IP_f = 150 V. This was a direct example of the effect of AC_{trap} on DP we have observed in the past. Overall, the preferential ejection of the highest m/z droplet upon increase of the target plate potential indicated that m/z was a factor in ejection order and hence the EDB essentially acted as a mass filter for the charged droplets.

There are two ways that WaSP could be used to filter droplets. The first would be to trap a population of droplets, anywhere from 1-50 droplets, in the EDB. Then, single droplets can be ejected from the balance onto a target based on their m/z, while the remaining droplets remain trapped. If desired, this stably levitated population could then be exposed to gas-phase reactants to modify their chemistry before their ejection, enabling experimental determination of their environment on the ability to identify them. The second approach would be to set up the EDB to act as a bandpass filter, allowing

only a certain range of m/z to pass through it, automatically ejecting the droplets in less than 500 ms. This method would be useful for rapidly sorting of droplets based on their m/z.

During the development of these modes of operation we used a translatable collection plate to make the demonstration clearer. In the first mode, the delayed ejection mode (Figure 11, mode 1), one droplet at a time was ejected from a *population* of droplets trapped in the EDB by using an attractive potential applied to the target plate. The position of the target plate relative to the EDB was changed in between each droplet ejection event, thereby creating an array of deposited droplets. Alternatively, a rapid ejection mode was developed (Figure 11, mode 2). Single droplets were created ($IP_f = 20$ V) at a frequency of 1 Hz while $AC_{trap} = 2700$ V with the potential applied to the collection plate set at 200 V. This caused each droplet to be briefly trapped in the EDB, allowing the methanol to evaporate. In <1 s each droplet escaped the electric field of the EDB and was ejected along the z axis at $x = y = 0$. By moving the collection plate between each droplet generation event, an array of deposited droplets was formed. The accuracy of droplet deposition using both methods, partially limited by the manual micrometer translation of the collection plate, has been measured by comparing the final position of the deposited droplets with their expected positions, yielding an average variation of ± 5 μm.**[131]** The flexibility of this basic procedure could be significantly expanded by introducing computerized control of the collection plate translation and the potentials applied to the EDB electrodes, all synchronized to the droplet generation event.

There are several aspects of WaSP charged droplet filtering that make it very flexible with respect to the types of application for which it could be used. First of all, the droplets that are filtered by WaSP are created from a starting solution of choice, therefore putting very little limitation on the potential analytes studied, such as single bacteria or synthetic inorganic particles. Next, the m/z of the droplets does not have to fit within the range that was demonstrated in this manuscript. By changing the characteristics of the electric field, WaSP can be easily modified to filter alternate m/z's. The source of the charged particles is also not limited to strictly charged droplet dispensers. Experiments are planned to explore the applicability of WaSP to filter atmospheric particles using alternate charging mechanisms. Lastly, the target for particle collection is not limited to a stainless steel plate. We have also delivered particles onto populations of cells on a glass slide and into the orifice of a mass spectrometer.

Overall, the flexibility of this charged particle filtering methodology based on WaSP has proven valuable in the development of such applications as the preparation of μm-sized sample spots for MALDI-TOF-MS and the study of multi-phase heterogeneous reactions on single aerosol particles. Some other potential applications of an using an EDB as a particle filter include: (1) a delivery module for a bioaerosol mass spectrometer attempting to detect single cells, bacteria, or viruses, (2) isolation of inorganic particles for subsequent studies based on their m/z, (3) an aerosol particle sorting mechanism, (4) a tool for performing studies of aerosol particle reactivity or nucleation capabilities based on their m/z, or (5) the single particle dosing of cell populations for medical research.

5.3 The effect of a charged MALDI plate on CHCA crystallization and ion production

The rationale for performing the experiments described in this section was to ascertain that the potential applied to the plate being used as the target for deposition of a levitated droplet/particle was not influencing the results.

In section 5.1, the nucleation of CHCA was described as being influenced by the mass-to-charge of the nucleation vessel. However, in all of those experiments, the extent of nucleation was not measured in situ (ie. in the levitated droplet) but rather only after the levitated droplet had been deposited on a target. The target was either a stainless steel plate to which a potential was applied to attract the levitated droplet or a glass cover slip positioned on top of the stainless steel plate to which a

potential was applied. To eliminate the possibility that the desposition of the droplet from the EDB onto a substrate was responsible for the observations made in section 5.1, we proceeded to pipette an aliquot of a stock solution onto a biased stainless steel plate. Note that in these experiments, even though the plate is charged, the droplet deposited onto it remained net neutral because within the droplet a double layer would be established immediately upon contact with the plate. So, even though the actual material deposited onto a plate in this section was a neutral droplet, and thus different from the deposition of a droplet with net charge, the effect of the deposition onto a biased plate on the nucleation of the dissolved solids was the objective of this section. In other words, the hypothesis was, does the drying of a droplet on a biased plate affect crystal formation and growth, and does that in turn affect signal-to-noise ratio (S/N) of the analytes contained in the droplet?

A stock solution of 10 pmol/μl of renin was prepared in distilled deionized water with 0.1 % trifluoroacetic acid. The MALDI matrix α-cyano-4-hydroxycinnamic acid (CHCA) was prepared at 10 mg/ml in 50:50 methanol:acetic acid. 10 μl of each solution was mixed in a microcentrifuge tube and vortexed. The MALDI plate was connected to a DC power supply of +500 V. Four 1 μl aliquots were deposited on to the MALDI plate as four discrete sample spots and allowed to air dry for 15 minutes. The MALDI plate was then grounded and four more 1 μl aliquots were deposited onto the MALDI plate and allowed to air dry for 15 minutes. Images of the sample spots were collected through an optical microscope at 4 and 10 times magnification (Figure 12). Mass spectra were then collected on a MALDI-TOF-MS in reflectron mode (M@LDI-LR, Waters Technologies Inc., Manchester, U.K.). The mass spectrometer was programmed to collect 10 mass spectra, comprised by the average of 10 laser shots, at 10 random positions within each sample spot at a fixed laser intensity. This procedure was repeated for five different laser intensities ranging from below to above the threshold required for ionization of the renin, the results of which are presented in Figure 13.

The plate onto which the sample was aliquotted using a micropipette was biased to 1000 V, and the experiment repeated. The analysis of the data acquired using MALDI-ToF-MS of the sample materials prepared on a grounded plate and a plate biased to 1000 V during the period that the droplets dried are presented in Figure 14.

Examination of the data presented in Figure 12, 13, and 14 indicate that the potential of the plate on which a droplet dries does affect the appearance of the crystals that result. This observation could be of use for crystal growth. However, the S/N of the analyte in the droplets is not significantly different from that obtained when a droplet is dried on a grounded plate.

6.0 POTENTIAL AREAS OF APPLICATION

- Control of the mass-to-charge of a nucleation vessel to assist in the nucleation and growth of crystals of dissolved solids. A dissolved solid could be any organic or inorganic compound, or any combinations thereof.
- Control of the mass-to-charge of a nucleation vessel to form nuclei which can then be used to seed a second nucleation vessel that has optimal conditions for crystal growth.
- Control of the mass-to-charge and chemical composition of a nucleation vessel to assist in the nucleation and growth of crystals of proteins. Specifically, the nucleation vessel that a has mass-to-charge can be further optimized through the use of, for example, various solvents which may or may not be miscible, another solute that can form nuclei, buffers.
- If droplets whose m/z spanned a range, then in a single experiment, the optimal m/z could be deduced via the ejection of the droplets onto a target (*ie.* a substrate such as a glass cover slip) that was held stationary during the deposition. By placing the ring electrodes at a small angle relative to the

surface of the target, it has been confirmed that droplets with different m/z can be deposited onto different regions of the target.

• Control the co-crystallization (rather than co-precipitation which implies aggregation) of a dissolved solid with a matrix for MALDI. Homogeneous co-crystallization could yield improved analytical performance of MALDI-TOF-MS when used to characterize sample materials.

6.1 Illustration of how this invention could be applied to the growth of crystals of a MALDI matrix within which an analyte compound co-precipitates.

Prior work from other groups has indicated that homogeneous co-crystallization of a solute with a matrix compound is a key criteria for obtaining good signal-to-noise (S/N) ratio for the analyte when characterized using MALDI-ToF-MS.[139] Furthermore, the quality of the crystals of a matrix that form on a surface has been characterized as heterogeneous.[140, 141] This body of information suggests that there is a need for methodology that enables for the formation of good quality crystals within which there is an analyte distributed homogeneously within that crystal in order to realize adequate analytical performance, such as analyte S/N, when characterized by MALDI-ToF-MS.

Several sets of experiments were performed in which droplets were created using different induction potentials. Each experiment was performed with a starting solution prepared daily with the following composition: 40 μL Acetone, 100 μL of a CHCA solution that was originally prepared by mixing 1:1 v:v acetonitrile:0.1% TFA in distilled deionized H_2O, 60 μL of water/glycerol solution that was originally prepared by mixing 1:4 glycerol:distilled deionized H_2O, 50 μL of ACTH solution with a concentration of 10 μM which makes the final concentration in the solution used for levitation 1 μM, and 150 μL Acetonitrile (ACTH = Adrenocorticotropic Hormone, Fragment 18-39). All droplets were levitated for a period of 5 minutes prior to their deposition onto a substrate remote from the EDB. The substrate was a stainless steel MALDI plate in this work.

The MALDI plate was then inserted into MALDI-ToF-MS (model Voyager, Perseptive Biosysems, MA) and the levitated droplet residues targeted by the laser and the mass spectra obtained are displayed in Figure 15-18.

Based on the data presented in these figures, the utility of a high induction potential during the droplet formation results in an improved S/N ratio for an analyte compound in the starting solution.

7.0 SUMMARY

We can exploit the mass-to-charge ratio of a volume of liquid, such as a droplet with net charge, to effect nucleation of its solutes, either organic, inorganic, or any combination thereof. In general, we can process compounds differently through changes in the mass-to-charge ratio of the droplet, or more generally, a vessel. The volume of liquid could also be a localized region in a conducting, semi-conducting, or non-conducting capillary, and one possible capillary could be a quartz or plastic or glass micro-machined or pull capillary. An important feature is that the charge-induced nucleation is being performed in the condensed phase (liquid phase). The droplet can be levitated or trapped using electrical, magnetic, acoustic, optical, or any combination thereof. Through controlled manipulation of the droplet mass-to-charge ratio, the rate of nucleation in the levitated droplet can be adjusted. Possible applications include seeding of a vessel with a crystal grown in a levitated droplet to effect crystal growth, enhancement of the rate of crystal nucleation and formation for organic compounds, and formation of small crystals in which organic or inorganic compounds, or any combination thereof, are co-crystallized.

8.0 LIST OF TABLES

Table 1. Results of the first experiment that unambiguously identified the droplet's mass-to-charge ratio as the experimental variable that was responsible for influencing the number of nuclei in a levitated droplet residue. The number of precipitates observed per droplet residue is indicated, but not that there was no differentiation between nuclei versus aggregates in this data set.

	Induction Potential (Volts)		
Droplet Number	**100**	**150**	**200**
1	0	2	1
2	0	7	>9
3	1	2	7
4	0	3	0
5	0	0	0
6	0	0	~45
7	3	0	0
8	0	3	5
9	1	5	2
10	1	2	2
11	5	5	8
12	0	2	1
13	2	3	6
14	4	2	4
15	2	5	10
16	0	4	0
17	0	0	3
Average	1	4	6

Table 2. The numbers of precipitates in each glycerol droplet are summarized in this table. Droplets were levitated under 100 and 180 V. There were 44 replicates performed using an induction potential of -100 V, and 8 replicates performed using an induction potential of -180 V. The crystals sizes observed were categorized as either >3.5 μm in diameter or 1.0-3.5 μm in diameter.

	Induction Potential (Volts) & Size of Solids (μm)					Induction Potential (Volts) & Size of Solids (μm)			
	-100 V		-180 V			-100 V		-180 V	
Replicate	>3.5	1.0-3.5	>3.5	1.0-3.5	Replicate	>3.5	1.0-3.5	>3.5	1.0-3.5
1	4	0	7	0	23	3	0		
2	0	7	8	10	24	3	0		
3	2	2	1	6	25	1	3		
4	3	0	2	9	26	3	1		
5	1	0	1	5	27	1	3		
6	2	0	8	32	28	3	3		
7	1	0	3	4	29	1	0		
8	3	0	8	36	30	6	2		
9	3	1			31	2	3		
10	4	0			32	1	1		
11	4	3			33	0	4		
12	2	0			34	1	0		
13	1	3			35	2	0		
14	1	2			36	1	0		
15	1	0			37	2	0		
16	2	0			38	1	0		
17	3	4			39	2	0		
18	3	0			40	2	0		
19	2	0			41	1	0		
20	4	1			42	2	0		
21	2	0			43	2	0		
22	3	1			44	2	4		
					Average	2	1	5	13

Table 3. Nuclei (either 1.0-3.5 μm in diameter or <1.0 μm in diameter) versus aggregates (agg) in levitated droplets as a function of the induction potential, either 100 or 190 V, used to induce net charge during the formation of each droplet. The number of replicates performed with an induction potential of 100 V and 190 V was 12 and 6 respectively.

Replicate	Induction Potential (Volts) and Solid Type or Crystal Size (μm)					
	100 V			190 V		
	agg	1.0-3.5	<1.0	agg	1.0-3.5	<1.0
1	1	0	0	0	2	1
2	1	0	0	0	1	2
3	2	0	0	0	0	0
4	0	0	0	0	0	0
5	0	0	0	0	1	0
6	1	0	0	0	0	0
7	0	0	0			
8	0	0	0			
9	0	0	0			
10	0	0	0			
11	0	0	0			
12	0	0	0			
Average	0.4	0	0	0	0.7	0.5

Table 4. The DC potential applied to the MALDI plate required to eject each droplet of a pair of droplets created with varied induction electrode potentials.

Induction potential applied during droplet formation (IP_f), volts		Potential applied to target plate (DP), volts		
1st	2nd	1st	2nd	ΔDP
Identical m/z pairs 50[a]	50[a]	58.6 ± 0.5	58.9 ± 0.3	0.3 ± 0.6
100[a]	100[a]	66.8 ± 1.9	69.1 ± 3.5	2.3 ± 4.0
150[b]	150[b]	91.7 ± 3.0	95.8 ± 4.7	4.1 ± 4.9
50[b]	50[b]	75.2 ± 0.9	76.3 ± 1.7	1.1 ± 2.3
Different m/z pairs 50[a]	100[a]	61.0 ± 1.0	72.0 ± 1.7	11 ± 2.0
50[b]	150[b]	75.4 ± 1.7	99.6 ± 0.7	24.2 ± 2.2

AC_{trap} = 1600 $V_{0\text{-}P.}$, (b) AC_{trap} = 2150 $V_{0\text{-}P.}$

9.0 LIST OF FIGURES

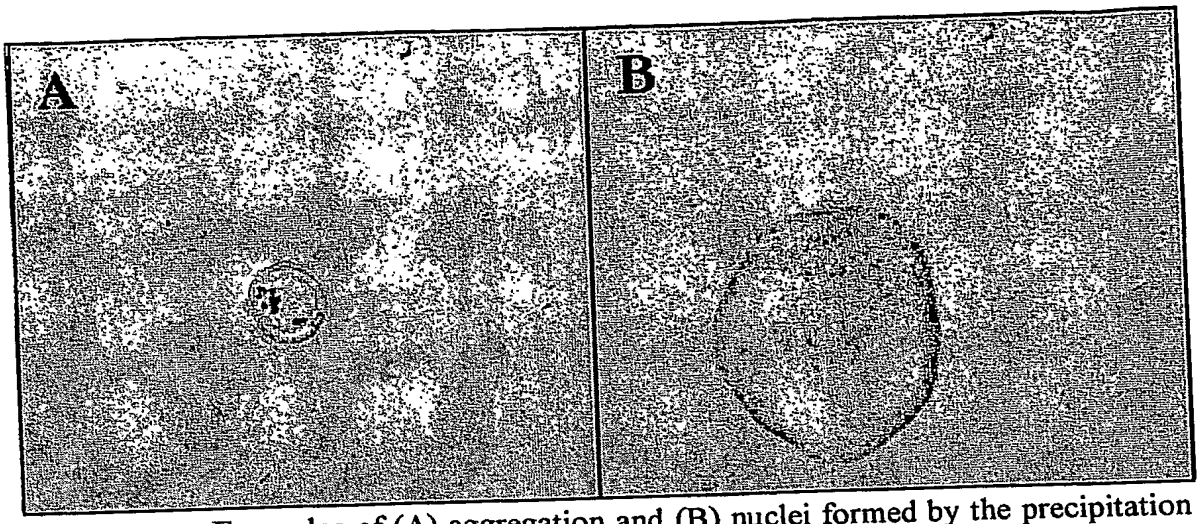

Figure 1. Examples of (A) aggregation and (B) nuclei formed by the precipitation of a dissolved solid. Notice the globular, dark appearance of the α-cyano-4-hydroxycinnamic acid (CHCA) aggregates versus the sharp edged, whiter in appearance crystals of CHCA, and this terminology to describe the solids formed in an experiment will be used throughout this application. The solids in these figures were formed and retained in glycerol, which is a liquid of low volatility and high viscosity.

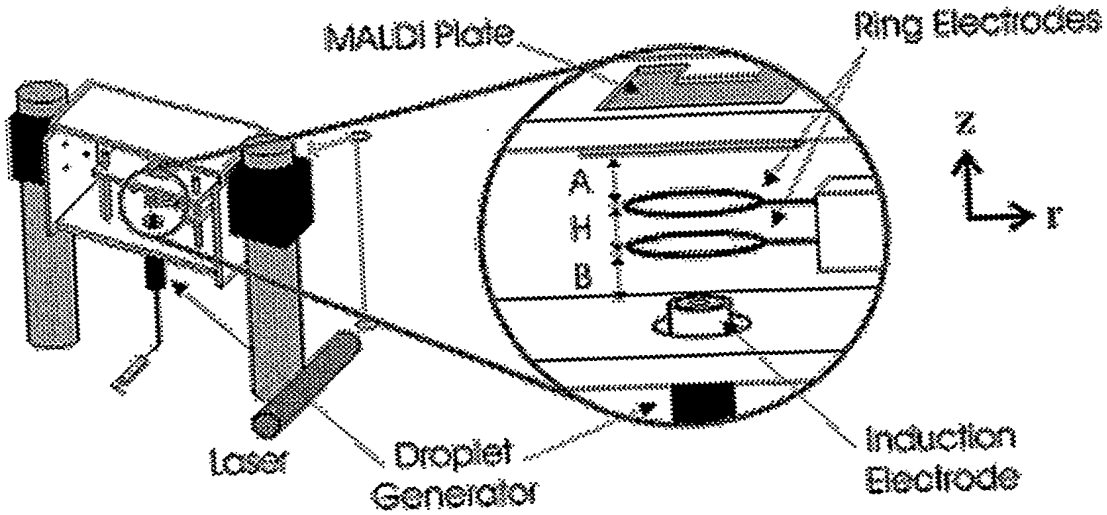

Figure 2. Depiction of the apparatus used for droplet generation, levitation, and deposition. This apparatus and its use to deposit levitated particles onto a target remote from the EDB which is described in patent PCT/CA01/01496 (W0 02/035553 A3)

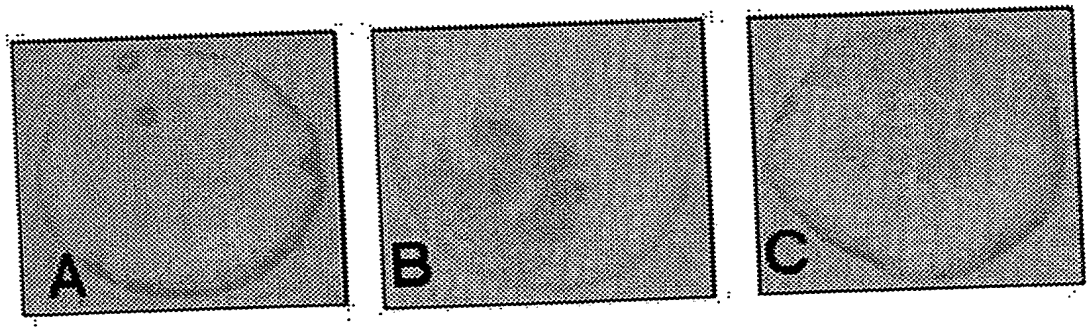

Figure 3. Pictures of deposited glycerol droplets that had been generated and levitated under the same conditions with the exception that the induction potential was 100, 150 and 200 V for a, b and c respectively. The actual number of crystals of CHCA in each of the residues, and particularly in Figure 3C, are not all in focus in these single pictures as the depth of view using the microscope optics was smaller than the depth of the glycerol residue in which the CHCA crystals were dispersed. The average size in micrometers of the residues for the conditions used were, A: 57.5 ± 8.8, B: 49.3 ± 4.6, and C: 57.5 ± 6.3.

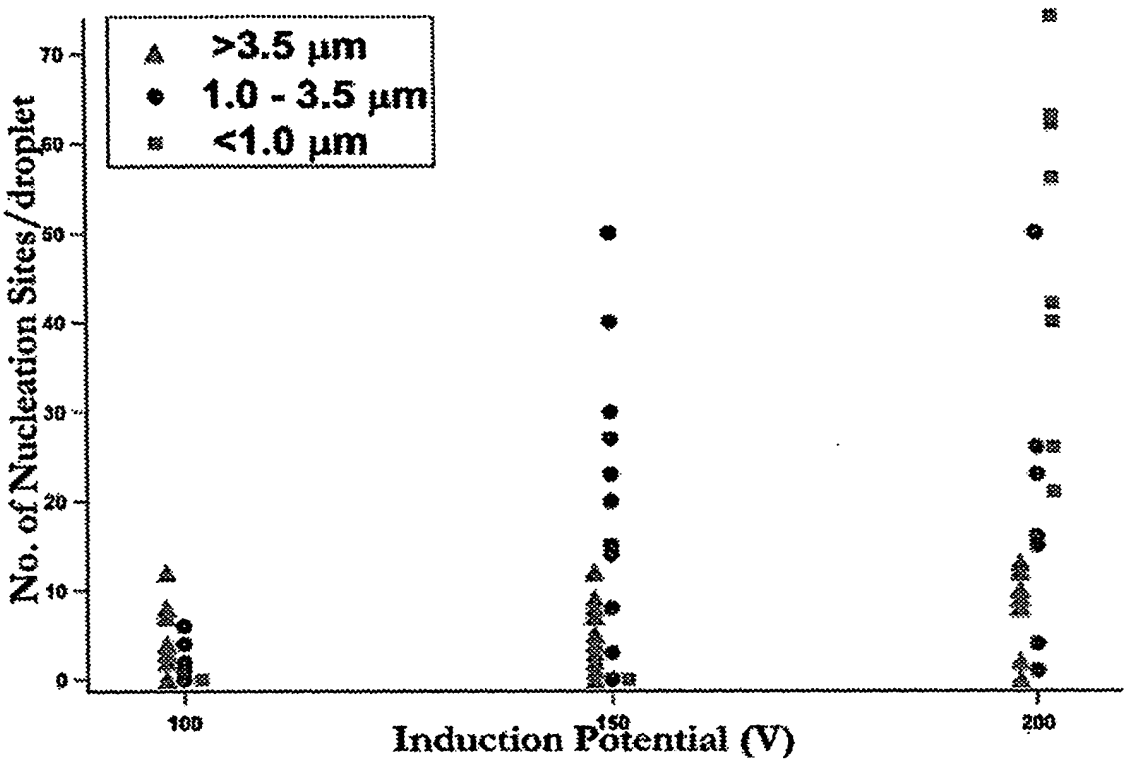

Figure 4. Number of nucleation crystals of CHCA (= α-cyano-4-hydroxycinnamic acid) in levitated glycerol residues as a function of the DC potential applied to the induction electrode. The residues of the levitated droplets were viewed using an optical microscope and the number of nucleation sites counted manually. The legend indicates the three symbols used to plot the number of crystals within each of the size ranges (diameter of crystal) counted in each droplet.

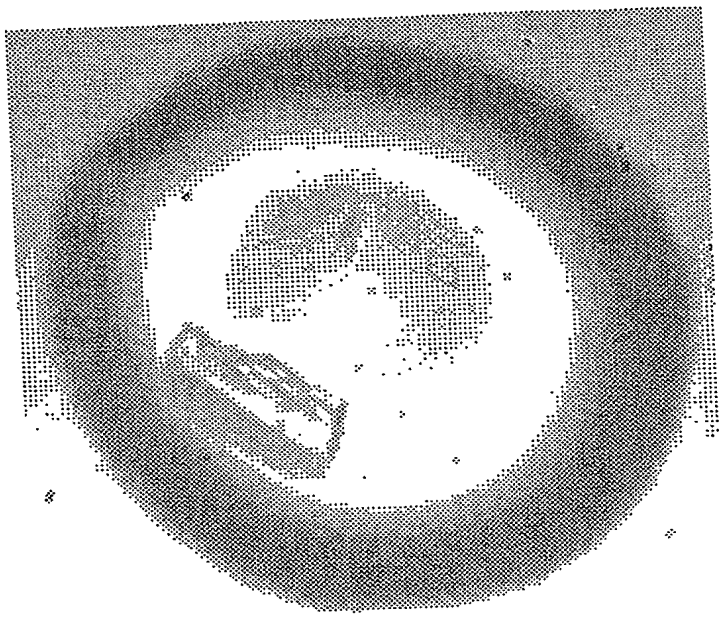

Figure 5. Picture of a glycerol droplet residue in which there was a single crystal of CHCA. The length of the crystal was 21 μm.

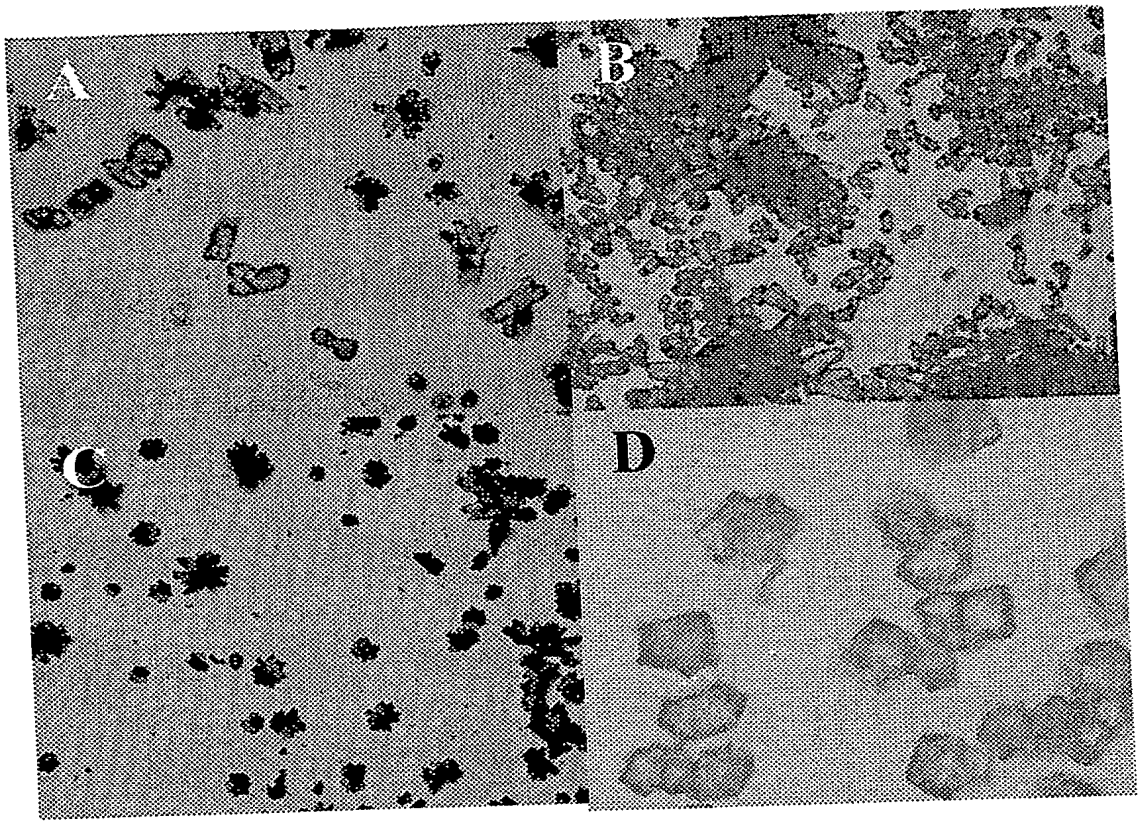

Figure 6. Pictures of CHCA solids (aggregates and crystals) created without (A, B, and C) and with (D) seeding using nuclei formed in a nucleation vessel with net charge (*ie*. a levitated droplet). See text for details.

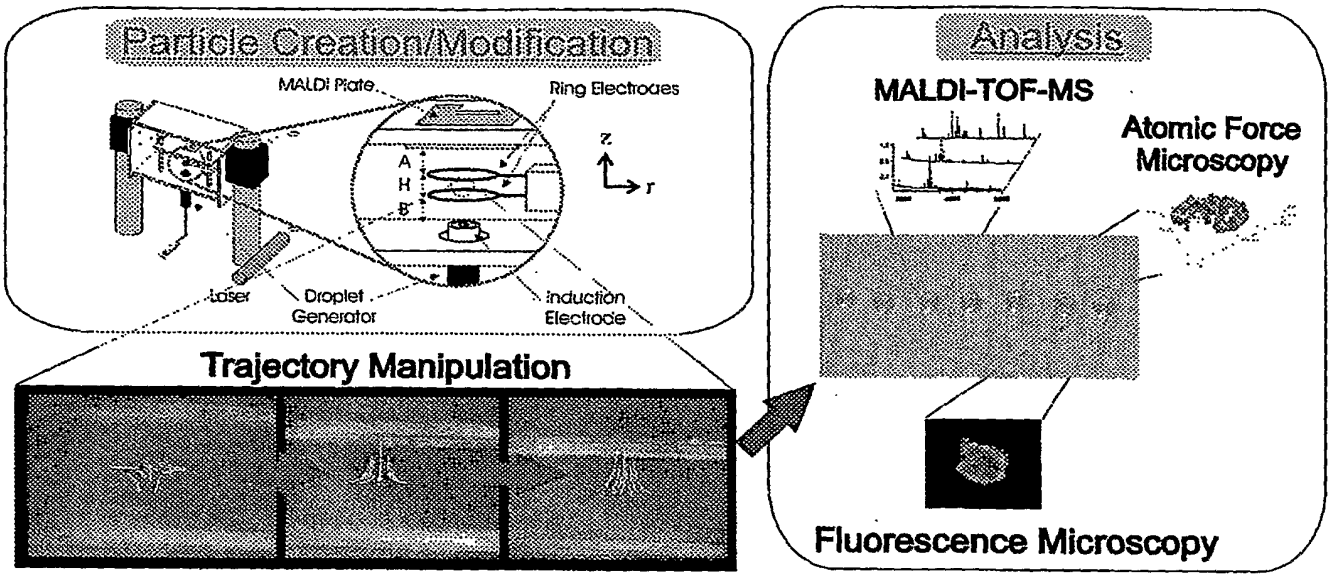

Figure 7. Wall-less Sample Preparation: the use of an electrodynamic balance to prepare and deliver μm-sized charged droplets to a target for subsequent analysis.

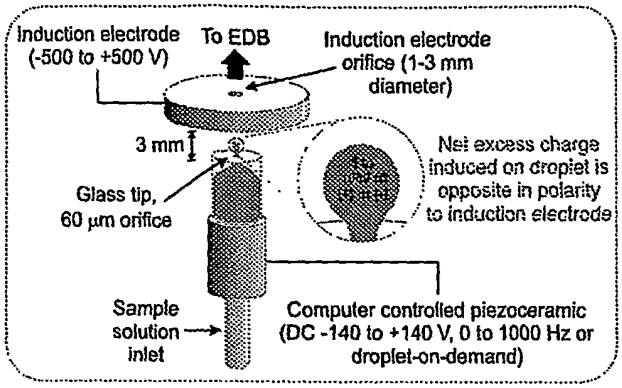

Figure 8. Apparatus for creating standard glycerol droplets carrying net excess charge.

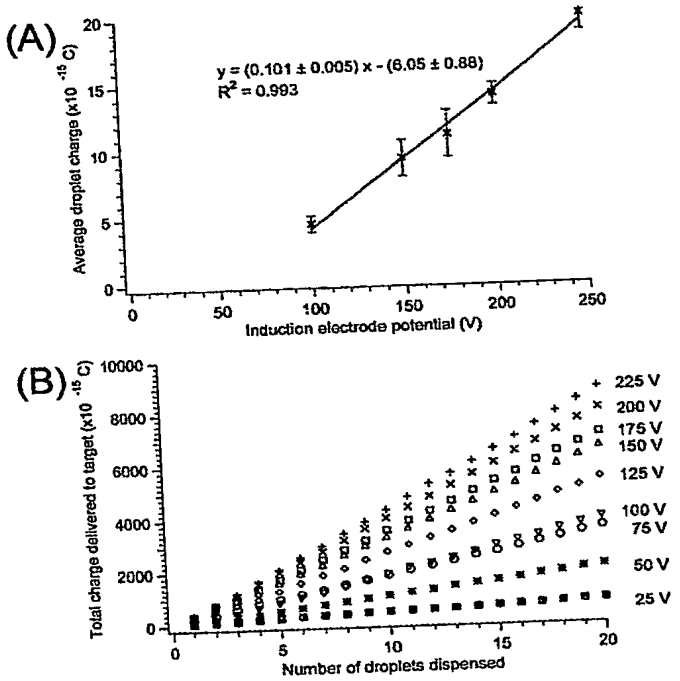

Figure 9. (A) The average net excess charge carried by a single droplet as a function of the amplitude of the DC potential applied to the induction electrode. All droplets were dispensed with ±10 V applied to the droplet dispenser piezoceramic and each data point is the average charge per droplet of 100 droplets dispensed at 100 Hz. (B) The total charge delivered to the target plate as a function of the number of droplets deposited onto the plate. The single droplets were dispensed at 0.5 Hz with ±30 V applied to the droplet dispenser piezoceramic. The amplitude of the DC potential applied to the induction electrode is noted next to each set of data points.

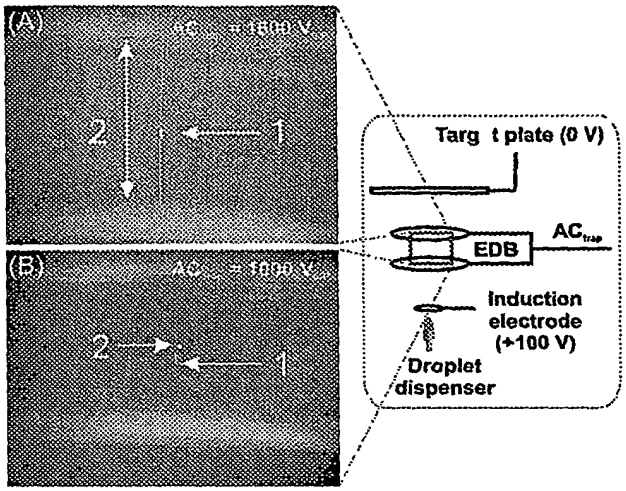

Figure 10. Digital images of pairs of glycerol droplets levitated in the EDB while the DC potential applied to the induction electrode was maintained at 100 V while AC_{trap} was set to (A) 1600 $V_{0\text{-}P}$ and (B) 1000 $V_{0\text{-}P}$. Droplet 1 was created with a higher m/z relative to droplet 2 by applying an IP_f of 50 V and 100 V, respectively. Also included is a depiction of the experimental apparatus to aid in the orientation and conditions under which the images were collected.

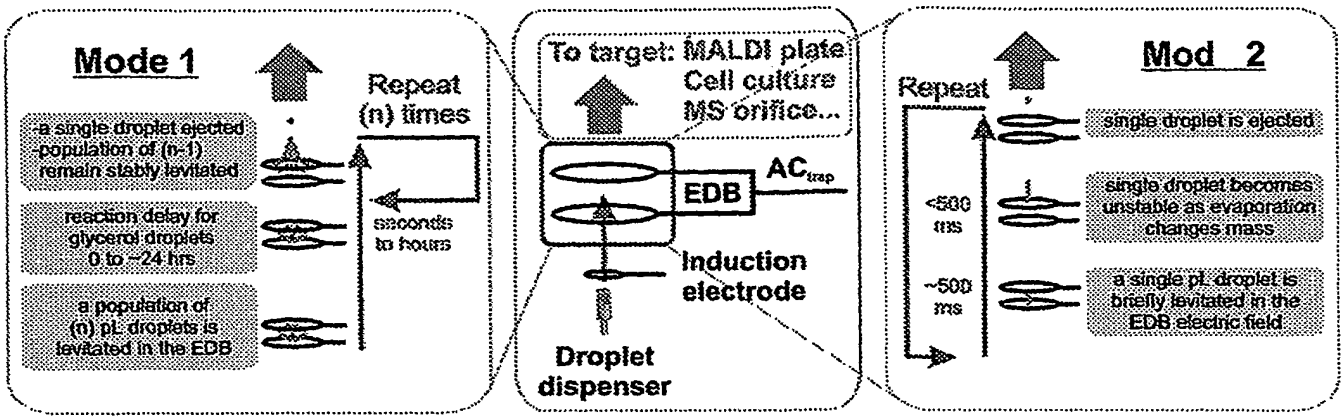

Figure 11. Illustration of the steps defining the two modes of operation of the WaSP-based charged particle filtering device for single particle delivery to a target.

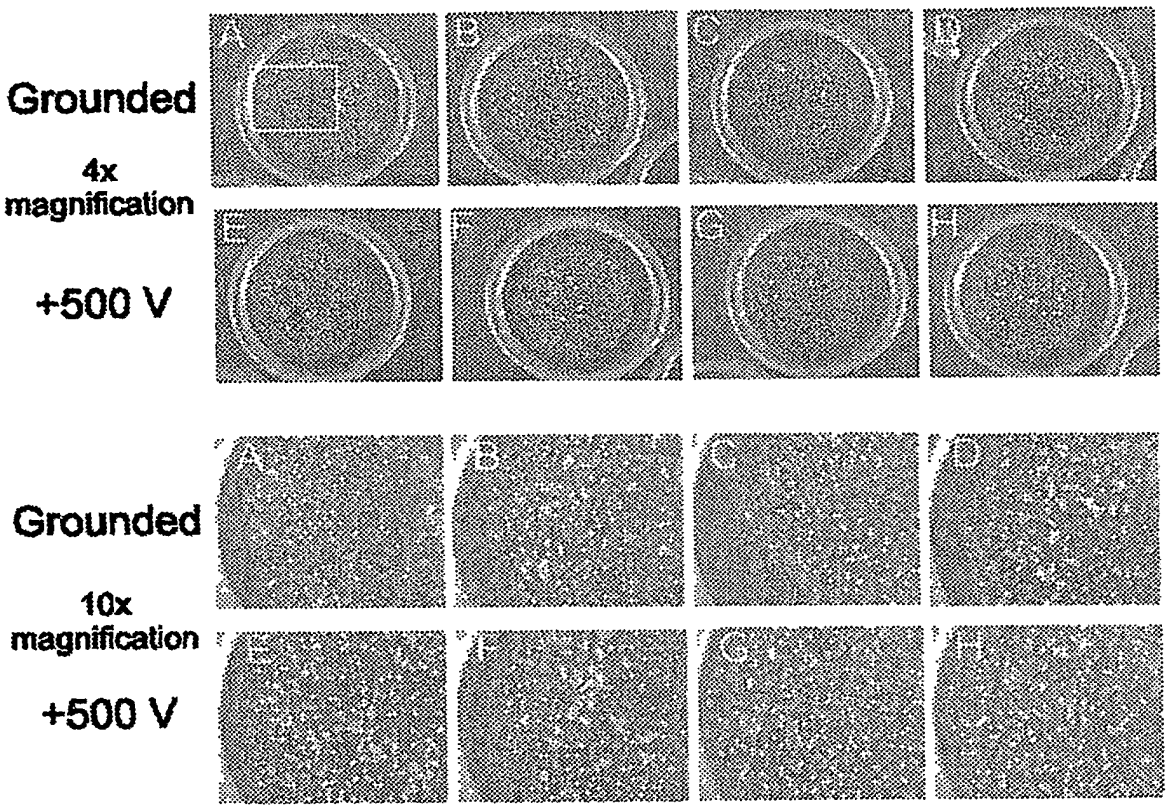

Figure 12. Eight MALDI sample spots created by depositing 4 aliquots of 1 µl CHCA/renin mixture (see text for details, section 5.3) onto the MALDI plate (A-D) grounded and (E-H) at +500 V DC. The white box denotes the area of each sample spot that was magnified to 10 times (bottom rows of images).

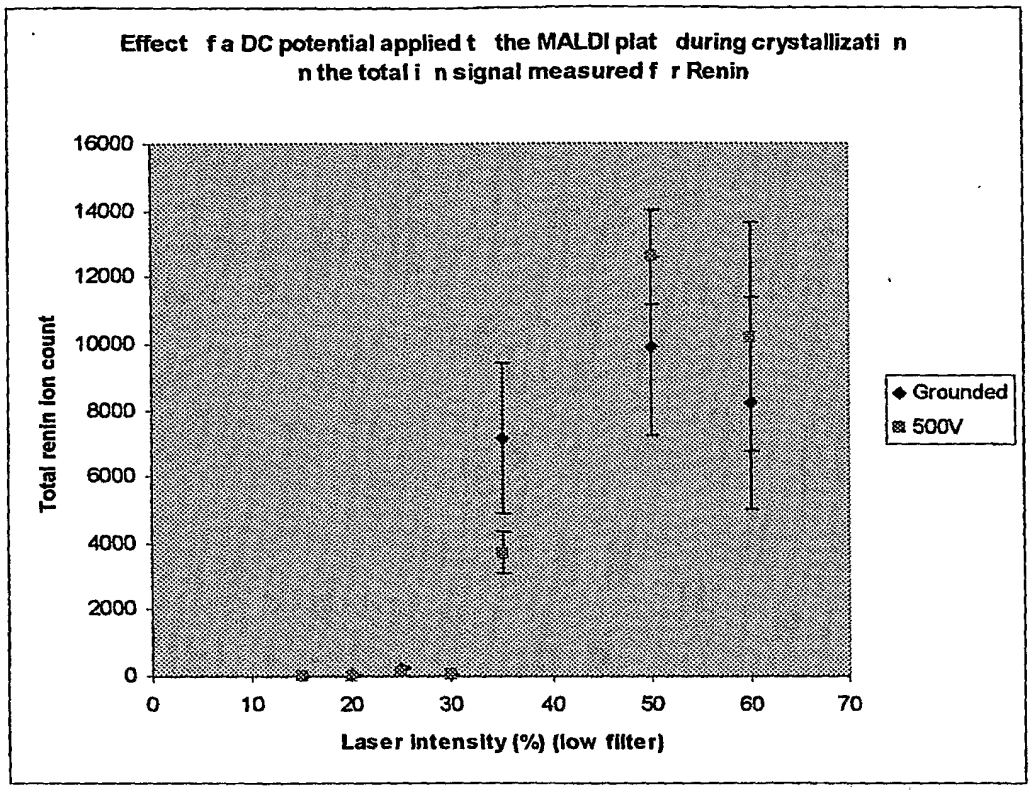

Figure 13. The total renin ion count (the sum of all ion intensity from 1760-1767 Da) measured from the sample spots prepared with a grounded and +500 V DC MALDI plate during crystallization.

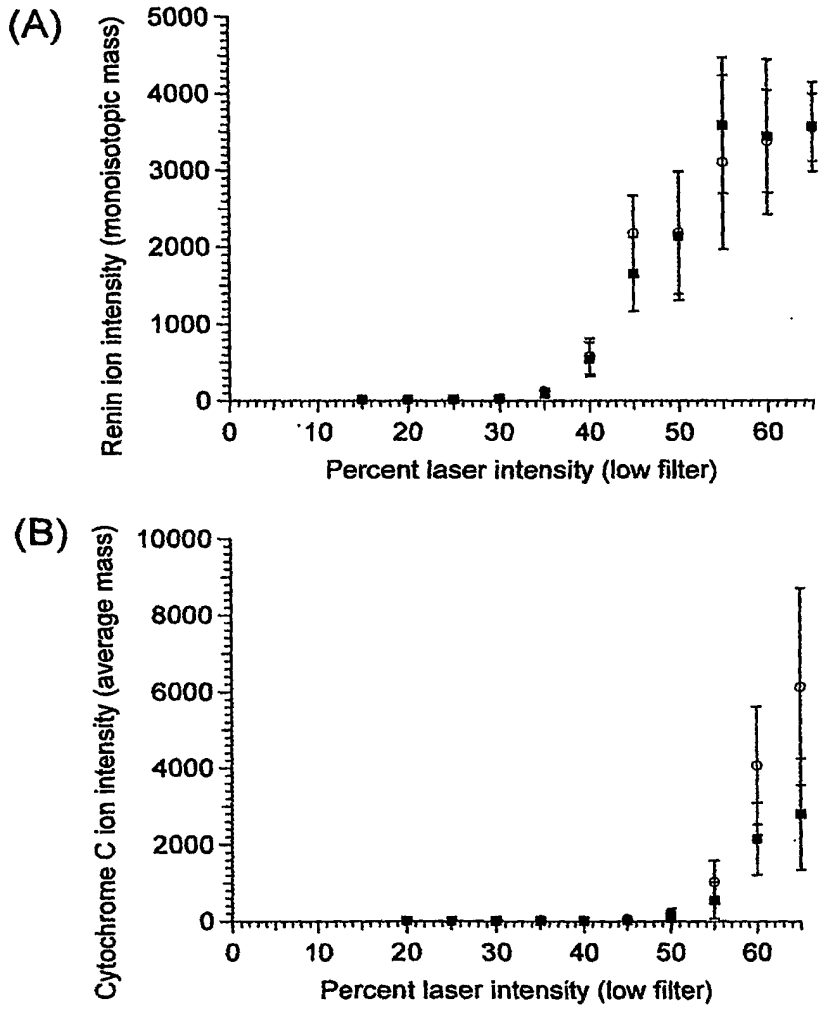

Figure 14. The effect of a DC potential applied to the MALDI plate during matrix crystallization on the ion intensity. Eight 1 μL aliquots of (A) a cytochrome C/sinapinic acid mixture or (B) a renin/α-cyano-4-hydroxycinnamic acid mixture were deposited onto a MALDI plate that was grounded (open circles) or had +5000 V DC applied to it (filled squares). Each data point represents the average of 800 laser shots collected as sets of 10 shots on 10 random positions for each of the eight sample spots.

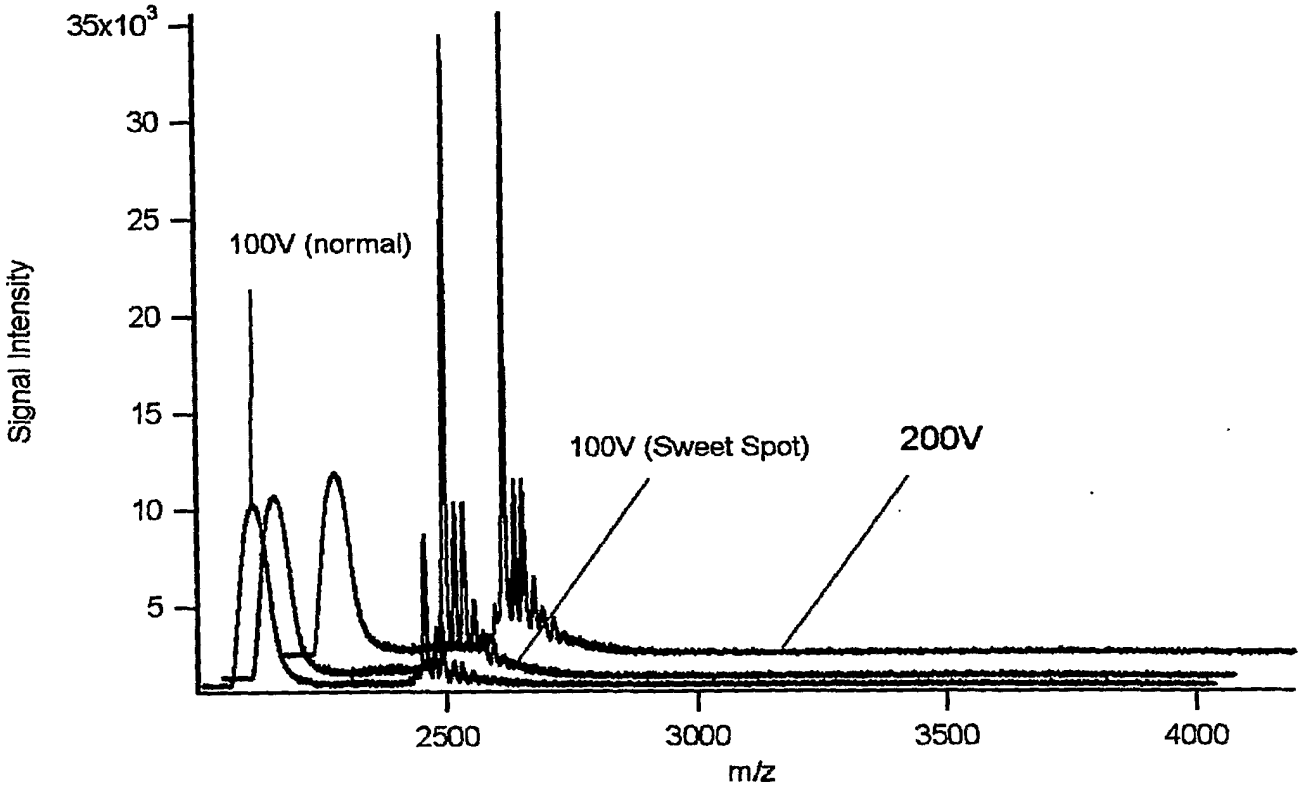

Figure 15. MALDI-ToF-MS spectra of ACTH from sets of 10 droplets, each created at 1 Hz using an induction potential of 100 or 200 V, and levitated in an EDB for 5 minutes. Each spectrum is the average of 8 laser shots acquired using a laser power setting of 4.47×10^{-4} J/shot. The spectrum identified by 'sweet spot' is SFB's terminology for what appeared to be rather good looking CHCA crystals in the residues of droplets that had been created at 100 V.

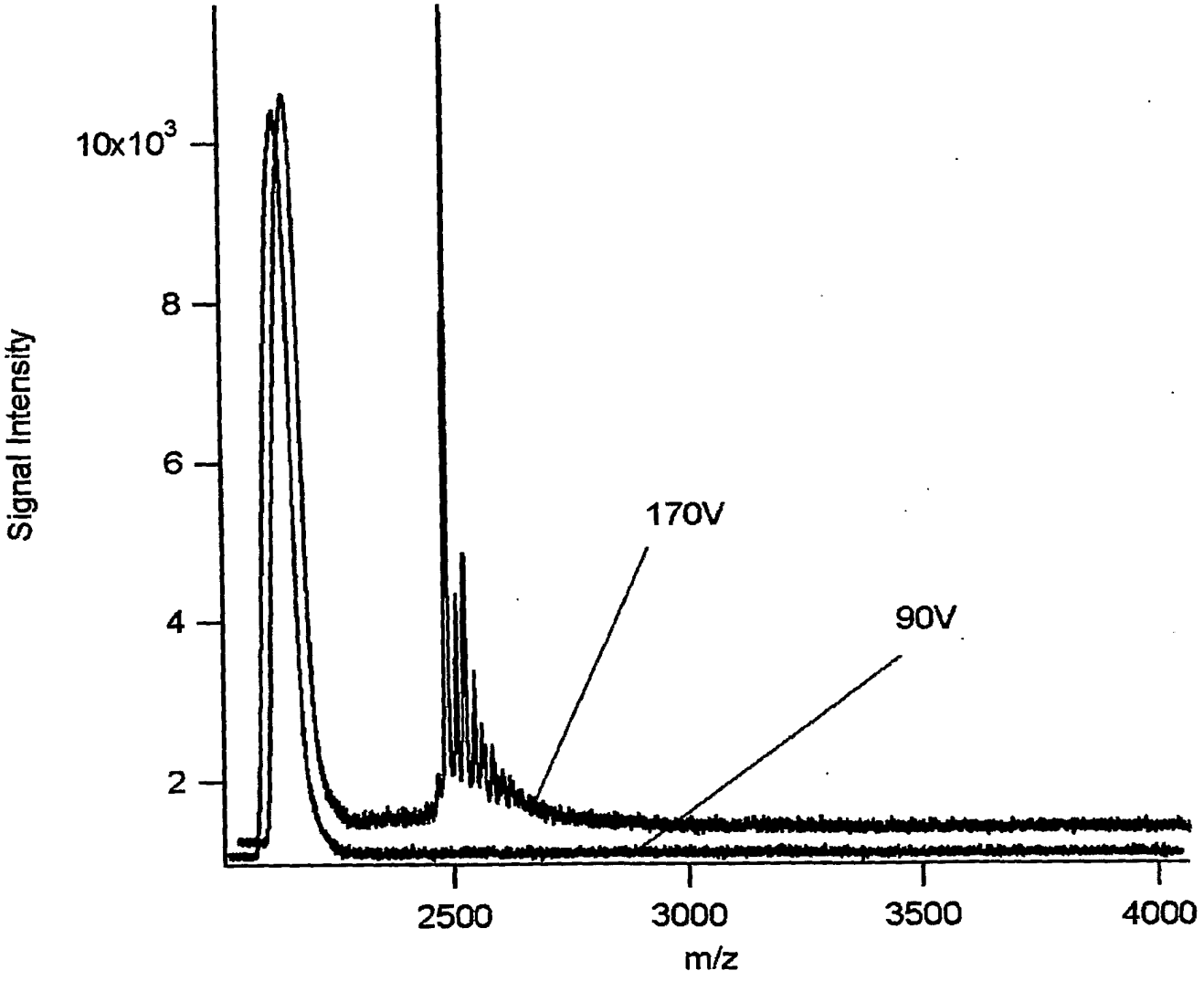

Figure 16. MALDI-ToF-MS spectra of ACTH from sets of 10 droplets, each created at 1 Hz using an induction potential of 90 or 170 V, and levitated in an EDB for 5 minutes. Each spectrum is the average of laser shot numbers 1-32, acquired using a laser power setting of 4.47×10^{-4} J/shot.

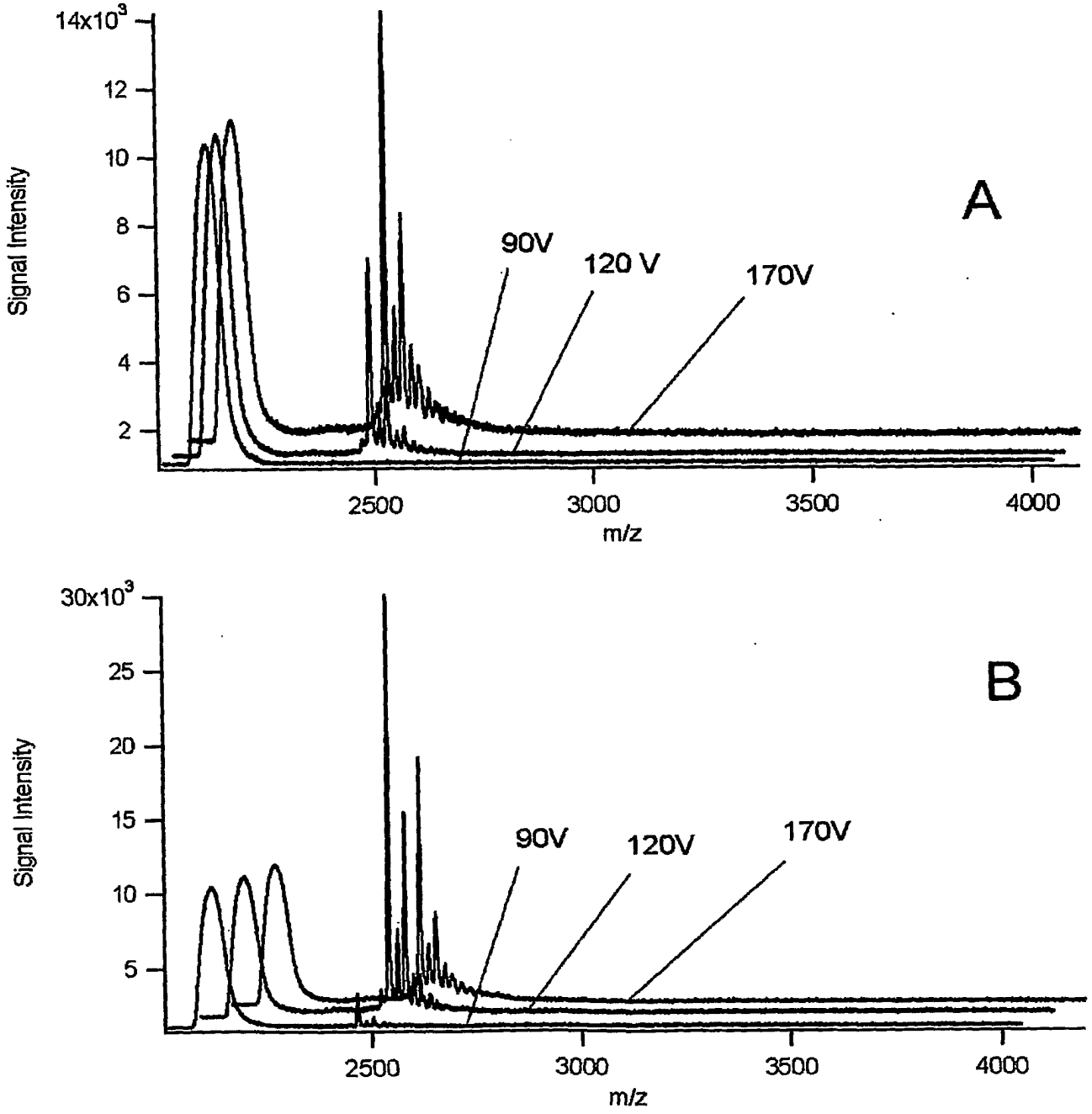

Figure 17. MALDI-ToF-MS spectra of ACTH from sets of 10 droplets, each created at 1 Hz using an induction potential of 90, 120, or 170 V, and levitated in an EDB for 5 minutes. The spectra are (A) the average of laser shot numbers 1-32, and (B) the average of laser shot numbers 33-64. All spectra were acquired using a laser power setting of 4.47×10^{-4} J/shot.

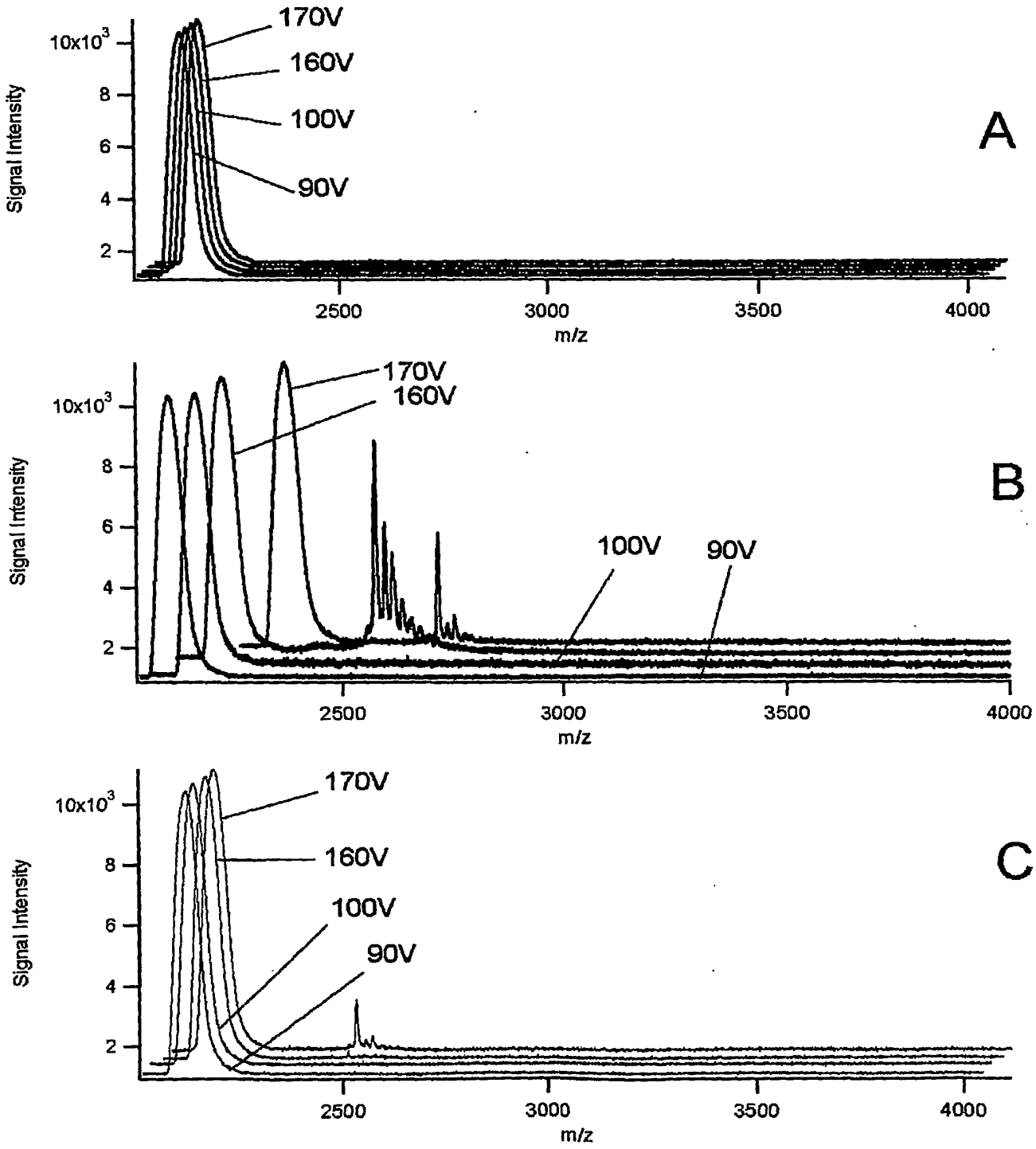

Figure 18. MALDI-ToF-MS spectra of ACTH from sets of 10 droplets, each created at 1 Hz using an induction potential of 90, 100, 160, or 170 V, and levitated in an EDB for 5 minutes. The spectra are (A) the average of laser shot numbers 1-32, and (B) the average of laser shot numbers 33-64, and (C) the average of laser shots 65-98. The spectra were acquired using a laser power setting of (A)

3.31x10^{-4} J/shot, (B) 4.47x10^{-4} J/shot, and (C) 3.31x10^{-4} J/shot.

10.0 REFERENCES

1. Bogan, M. J.; Agnes, G. R. MALDI-TOF-MS analysis of droplets prepared in an electrodynamic balance: "Wall-less" sample preparation *Anal. Chem.* 2002, *74*, 489-496.
2. Gao, J.; Volkmann, T.; Herlach, D. M. Solidification of levitated Nd-Fe-B alloy droplets at significant bulk undercoolings *J. Alloys Compounds* 2003, *350*, 344-350.
3. Croat, T. K.; Kelton, K. F.; Holland-Moritz, D.; Rathz, T. J.; Robinson, M. B. Containerless solidification studies of the _-1/1 crystal approximant in Ti-Cr-Si-O alloys *J. Mater. Res.* 1999, *14*, 4208-4213.
4. Bertero, G. A.; Hofmeister, W. H.; Robinson, M. B.; Bayuzick, R. J. Containerless processing and rapid solidification of niobium-silicon alloys of hypereutectic composition *Metallurgical Transactions A: Physical Metallurgy and Materials Science* 1991, *22A*, 2723-2732.
5. Nagashio, K.; Li, M.; Kuribayashi, K. Containerless solidification and net shaping by splat quenching of undercooled Nd2Fe14B melts *Materials Transactions* 2003, *44*, 853-860.
6. Hermann, R.; Bacher, I.; Matson, D. M.; Loser, W.; Schultz, L. Growth kinetics in levitated and quenched Nd-Fe-B alloys *IEEE Trans. Magn.* 2001, *37*, 1100-1105.
7. Nagashio, K.; Kuribayashi, K.; Takamura, Y. Direct crystallization of Y3Fe5O12 garnet by containerless solidification processing *Materials Transactions* 2001, *42*, 233-237.
8. Jacob, K. T.; Hajra, J. P. Electromagnetic levitation study of sulfur in liquid iron, nickel, and iron-nickel alloys *Trans. Indian Inst. Met.* 1986, *39*, 62-69.
9. Haddrell, A. E.; Agnes, G. R. Organic Cation Distributions in the Residues of Levitated Droplets with Net Charge: Validity of the Partition Theory for Droplets Produced by an Electrospray *Anal. Chem.* 2004, *76*, 53-61.
10. Keesee, R. G.; Castleman, A. W. Thermochemical data on gas-phase ion-molecule accosiation and clustering reactions *J. Phys. Chem. Ref. Data* 1986, *15*, 1011-.
11. Wells, J. M.; Chrisman, P. A.; McLuckey, S. A. Formation of protein-protein complexes in vacuo *J. Am. Soc. Chem.* 2001, *123*, 12428-12429.
12. Jang, H. M.; Hwang, N. M. Theory of the charged cluster formation in the low pressure synthesis of diamond: Part 1. Charge-induced nucleation *J. Mater. Res.* 1998, *13*, 3527-3535.
13. Jang, H. M.; Hwang, N. M. Theory of the charged cluster formation in the low pressure synthesis of diamond: Part II. Free energy function and thermodynamic stability *J. Mater. Res.* 1998, *13*, 3536-3549.
14. Snyder, T. D.; Richardson, C. B. A study of the nucleation of the solution-to-solid phase transition using levitated microscopic particles *Langmuir* 1993, *9*, 347-351.
15. Krämer, B.; Hübner, O.; Vortisch, H.; Wöste, L.; Leisner, T.; Schwell, M.; Rühl, E.; Baumgärtel, H. Homogeneous nucleation rates of supercooled water measured in single levitated microdroplets *J. Chem. Phys.* 1999, *111*, 6521-6527.
16. Li, D.; Herlach, D. M. High undercooling or bulk molten silicon by containerless processing *Europhys. Lett.* 1996, *34*, 423-428.
17. Krieger, U. K.; Colberg, C. A.; Weers, U.; Koop, T.; Peter, T. H. Supercooling of single H2SO4/H2O aerosols to 158 K: No evidence for the occurrence of the octrahydrate *Geophys. Res. Lett.* 2000, *27*, 2097-2100.
18. Anders, K.; Roth, N.; Frohn, A. New technique for investigating phase transition processes of optically levitated droplets consisting of water and sulfuric acid *J. Geophys. Res., [Atmos.]* 1996, *101*, 19223-19229.
19. Tang, I. N.; Munkelwitz, H. R. J. o. C. a. I. S.; (1984), 430-8. An investigation of solute nucleation in levitated solution droplets *J. Colloid Inter. Sci.* 1984, *98*, 430-438.

20. Vortisch, H.; Kramer, B.; Weidinger, I.; Woste, L.; Leisner, T.; Schwell, M.; Baumgartel, H.; Ruhl, E. Homogeneous freezing nucleation rates and crystallization dynamics of single levitated sulfuric acid solution droplets *Phys. Chem. Chem. Phys.* 2000, *2*, 1407-1413.
21. Weidinger, I.; Klein, J.; Stoeckel, P.; Baumgaertel, H.; Leisner, T. Nucleation Behavior of n-Alkane Microdroplets in an Electrodynamic Balance *J. Phys. Chem. B* 2003, *107*, 3636-3643.
22. Musick, J.; Popp, J. Investigations of chemical reactions between single levitated magnesium chloride microdroplets with SO2 and NOx by means of Raman spectroscopy and elastic light scattering *Phys. Chem. Chem. Phys.* 1999, *1*, 5497-5502.
23. Musick, J.; Kiefer, W.; Popp, J. Chemical reactions of single levitated inorganic salt particles with ammonia gas *Appl. Spectrosc.* 2000, *54*, 1136-1141.
24. Aardahl, C. L.; Davis, E. J. Gas/aerosol chemical reactions in the NaOH-SO2-H2O system *Appl. Spectrosc.* 1996, *50*, 71-77.
25. Aardahl, C. L.; Davis, E. J. Raman spectroscopy studies of reactions between sulfur dioxide and microparticles of hydroxides *Mater. Res. Soc. Symp. Proc.* 1997, *432*, 209-220.
26. Trunk, M.; Popp, J.; Hartmann, I.; Lankers, M.; Urlaub, E.; Kiefer, W. Chemical composition and reaction analysis of single aerosol particles *Fresenius' J. Anal. Chem.* 1996, *355*, 354-356.
27. Lamb, D.; Moyle, A. M.; Brune, W. H. The environmental control of individual aqueous particles in a cubic electrodynamic levitation system *Aerosol Sci. Technol.* 1996, *24*, 263-278.
28. Kim, Y. P.; Pun, B. K.-L.; Chan, C. K.; Flagan, R. C.; Seinfeld, J. H. Determination of water activity in ammonium sulfate and sulfuric acid mixtures using levitated single particles *Aerosol Sci. Technol.* 1994, *20*, 275-284.
29. Li, W.; Rassat, S. D.; Foss, W. R.; Davis, E. J. Formation and properties of aerocolloidal TiO2-coated microspheres produced by alkoxide droplet reaction *J. Colloid Interface Sci.* 1994, *162*, 267-278.
30. Davis, E. J.; Rassat, S. D.; Foss, W. Measurement of aerosol/gas reaction rates by microparticle Raman spectroscopy *J. Aeosol Sci.* 1992, *23*,
31. Rassat, S. D.; Davis, E. J. Chemical reaction of sulfur dioxide with a calcium oxide aerosol particle *J. Aerosol Sci.* 1992, *23*, 165-180.
32. Carls, J. C.; Moncivais, G.; Brock, J. R. Time-resolved Raman spectroscopy from reacting optically levitated microdroplets *Appl. Opt.* 1990, *29*, 2913-2918.
33. Davis, E. J. Optical measurements of electrodynamically levitated microparticles *Proc. SPIE-Int. Soc. Opt. Eng.* 1991, *1435(Opt. Methods Ultrasensitive Detect. Anal.: Tech. Appl.)*, 216-243.
34. Spann, J. F.; Richardson, C. B. Measurement of the water cycle in mixed ammonium acid sulfate particles *Atmos. Environ.* 1985, *19*, 819-825.
35. Widmann, J. F.; Aardahl, C. L.; Davis, E. J. Microparticle Raman spectroscopy *Trends Anal. Chem.* 1998, *17*, 339-345.
36. Jacob, P.; Stockhaus, A.; Hergenroder, R.; Klockow, D. Phase transfer and freezing processes investigated on acoustically levitated aqueous droplets *Fresnius' J. Anal. Chem.* 2001, *371*, 726-733.
37. Trunk, M.; Popp, J.; Lankers, M.; Kiefer, W. Microchemistry: Time dependence of an acid-base reaction in a single optically levitated microdroplet *Chem. Phys. Lett.* 1997, *264*, 233-237.
38. Esen, C.; Kaiser, T. Raman investigation of photopolymerization reactions of single optically levitated microparticles *Appl. Spectrosc.* 1996, *50*, 823-828.
39. Musick, J.; Popp, J.; Trunk, M.; Kiefer, W. Investigations of radical polymerization and copolymerization reactions in optically levitated microdroplets by simultaneous Raman spectroscopy, Mie scattering, and radiation pressure measurements *Appl. Spectrosc.* 1998, *52*, 592-701.
40. Ward, T. L.; Zhang, S. H.; Allen, T.; Davis, E. J. Photochemical polymerization of acrylamide aerosol particles *J. Colloid Interface Sci.* 1987, *118*, 343-355.
41. Widmann, J. F.; Davis, E. J. Photochemical initiated polymerization of single microdroplets *Colloid Polym. Sci.* 1996, *274*, 525-531.

42. Widmann, J. F.; Aardahl, C. L.; Johnson, T. J.; Davis, E. J. Encapsulation of levitated nicroparticles *J. Colloid Interface Sci.* 1998, *199*, 197-205.
43. Cederfelt, S.-I.; Martinsson, B. G.; Hansson, H.-C. On the charge limit for crystallizing particles 4. *Aerosol Sci.* 1990, *21*, S127-S130.
44. Rayleigh, L. *Philos. Mag.* 1882, *14*, 184-186.
45. Taflin, D. C.; Ward, T. L.; Davis, E. J. Electrified droplet fission and the Rayleigh limit *Langmuir* 1989, *5*, 376-384.
46. Smith, J. N.; Flagan, R. C.; Beauchamp, J. L. Droplet evaporation and discharge dynamics in electrospray ionization *J. Phys. Chem. A* 2002, *106*, 9957-9967.
47. Dudek, D. R.; Wright, D. A.; Longwell, J. P.; Sarofim, A. F.; Yeheskel, J. Charge loss from heated particles levitated in an electrodynamic balance *Combust. Sci. Technol.* 1990, *73*, 447-461.
48. Duft, D.; Achtzehn, T.; Muller, R.; Huber, B. A.; Leisner, T. Rayleigh jets from levitated microdroplets *Nature* 2003, *421*, 128.
49. Manil, B.; Ntamack, G. E.; Lebuis, H.; Huber, B. A.; Duft, D.; Leisner, T.; Chandezon, F.; Guet, C. Charge emission and decay dynamics of highly charged clusters and micro-droplets *Nucl. Instrum. Methods Phys. Res. B* 2003, *205*, 684-689.
50. Duft, D.; Lebuis, H.; Huber, B. A.; Guet, C.; Leisner, T. Shape oscillations and stability of charged microdroplets *Phys. Rev. Lett.* 2002, *89*, 84503.
51. Feng, X.; Bogan, M.; Agnes, G. R. Coulomb fission event resolved progeny droplet production from isolated evaporating methanol droplets *Anal. Chem.* 2001, *73*, 4499-4507.
52. Grimm, R. L.; Beauchamp, J. L. Evaporation and discharge dynamics of highly charged droplets of heptane, octane, and p-xylene generated by electrospray ionization *Anal. Chem.* 2002, *74*, 6291-6297.
53. Fenn, J. B.; Mann, M.; Meng, C. K.; Wong, S. F.; Whitehouse, C. M. Electrospray ionization for mass spectrometry of large biomolecules *Science* 1989, *246*, 64-71.
54. Kebarle, P.; Tang, L. From ions in solution to ions in the gas phase - the mechanism of electrospray mass spectrometry *Anal. Chem.* 1993, *65*, 972A-986A.
55. Constantopoulos, T. L.; Jackson, G. S.; Enke, C. G. Challenges in achieving a fundamental model for ESI *Anal. Chim. Acta* 2000, *406*, 37-52.
56. Gamero-Castano, M.; Fernandez de la Mora, J. Mechanisms of electrospray ionization of singly and multiply charged salt clusters *Anal. Chim. Acta* 2000, *406*, 67-91.
57. Gamero-Castano, M.; Fernadez de la Mora, J. Modulations in the abundance of salt clusters in electrosprays *Anal. Chem.* 2000, *72*, 1426-1429.
58. Wang, G.; Cole, R. B. Charged residue versus ion evaporation for formation of alkali metal halide cluster ions in ESI (Electrospray ionization) *Anal. Chim. Acta* 2000, *406*, 53-65.
59. Kojima, T.; Kudaka, I.; Asakawa, T.; Akiyama, R.; Kawashima, Y.; Hiraoka, K. Observation of triply charged metal ion clusters by electrospray and laser spray *Rapid Commun. Mass Spectrom.* 1999, *13*, 2090-2097.
60. Wang, G.; Cole, R. B. Solvation Energy and Gas-Phase Stability Influences on Alkali Metal Cluster Ion Formation in Electrospray Ionization Mass Spectrometry *Anal. Chem.* 1998, *70*, 873-881.
61. Zhou, S.; Hamurger, M. Formation of sodium cluster ions in electrospray mass spectrometry *Rapid Commun. Mass Spectrom.* 1996, *10*, 797-800.
62. Schalley, C. A.; Weis, P. Unusually stable magic number clusters of serine with a surprising preference for homochirality. *Int. J. Mass Spectrom.* 2002, *221*, 9-19.
63. Koch, K. J.; Aggerholm, T.; Nanita, S. C.; Cooks, R. G. Clustering of nucleobases with alkali metals studied by electropsray ionization tandem mass spectrometry: implications for mechanisms of multistrand DNA stabilization *J. Mass Spectrom.* 2002, *37*, 676-686.
64. Vrkic, A. K.; O'Hair, R. A. J. Gas phase ion chemistry of para substituted benzene diazonium ions, their salt clusters and their related phenyl cations *Int. J. Mass Spectrom.* 2002, *218*, 131-160.

65. Tao, W. A.; Cooks, R. G. Chiral preferences in the dissociation of homogeneous amino acid/metal ion clusters *Europ. J. Mass Spectrom.* 2002, *8*, 107-115.
66. Carlesso, V.; Fournier, F.; Afonso, C.; Tabet, J. C. Halogen counter-ion effect on the dissociation of monosaccharide-iron complexes generated by electrospray ionization combined with an ion trap mass spectrometer *Eur. J. Mass Spectrom.* 2001, *7*, 331-341.
67. Gaumet, J. J.; Strouse, G. Nanospray mass spectrometry technique for analysing nanomaterials from molecular precursors up to 1.5 nm in diameter cluster *Materials Science & Engineering C: Biomimetic and Supramolecular Systems* 2002, *C19*, 299-304.
68. Counterman, A. E.; Clemmer, D. E. Magic number clusters of serine in the gas phase *J. Phys. Chem. B* 2001, *105*, 8092-8096.
69. Hernandez, H.; Hewitson, K. S.; Roach, P.; Shaw, N. M.; Baldwin, J. E.; Robinson, C. V. Observation of the Iron-Sulfur Cluster in Escherichia coli Biotin Synthase by Nanoflow Electrospray Mass Spectrometry *Anal. Chem.* 2001, *73*, 4154-4161.
70. Hao, C.; March, R. E.; Croley, T. R.; Smith, J. C.; Rafferty, S. P. Electrospray ionization tandem mass spectrometry study of salt cluster ions. Part 1- investigations of alkali metal chloride and sodium salt cluster ions *J. Mass Spectrom.* 2001, *36*, 79-96.
71. Hao, C.; March, R. E. Electrospray ionization tandem mass spectrometric study of salt cluster ions: part 2 - Salts of polyatomic acid groups and of multivalent metals *J. Mass Spectrom.* 2001, *36*, 509-521.
72. Lee, Y.; Jo, S.-C.; Tao, W. A.; Cooks, R. G. Metal-assisted esterification: glutaric acid-iron(II) complexes in the gas phase *Rapid Commun. Mass Spectrom.* 2001, *15*, 484-488.
73. Lee, S.-W.; Cox, H.; Goddard, W. A., III; Beauchamp, J. L. Chemistry in Nanodroplets: Studies of Protonation Sites of Substituted Anilines in Water Clusters Using FT-ICR *J. Am. Chem. Soc.* 2000, *122*, 9201-9205.
74. Gamero-Castano, M.; De la Mora, J. F. Kinetics of small ion evaporation from the charge and mass distribution of multiply charged clusters in electrosprays *J. Mass Spectrom.* 2000, *35*, 790-803.
75. Zhang, D.; Wu, L.; Koch, K. J.; Cooks, R. G. Arginine clusters generated by electrospray ionization and identified by tandem mass spectrometry *Eur. Mass Spectrom.* 1999, *5*, 353-361.
76. Zhang, D.; Cooks, R. G. Doubly charged cluster ions [(NaCl)m(Na)2]2+: magic numbers, dissociation, and structure *Int. J. Mass Spectrom.* 2000, *195/196*, 667-684.
77. Charles, L.; Pepin, D.; Gonnet, F.; Tabet, J.-C. Effects of liquid phase composition on salt cluster formation in positive ion mode electrospray mass spectrometry: implications for clustering mechanism in electrospray *J. Am. Soc. Mass Spectrom.* 2001, *12*, 1077-1084.
78. Gamero-Castano, M.; de la Mora, J. F. Ion-induced nucleation: Measurement of the effect of embryo's size and charge state on the critical supersaturation *J. Chem. Phys.* 2002, *117*, 3345-3353.
79. Festag, R.; Alexandratos, S. D.; Cook, K. D.; Joy, D. C.; Annis, B.; Wunderlich, B. Single- and few-chain polystyrene particles by electrospray *Macromolecules* 1997, *30*, 6238-6242.
80. Green, B. N.; Gotoh, T.; Suzuki, T.; Zal, F.; Lallier, F. H.; Toulmond, A.; Vinogradov, S. N. Observation of large, non-covalent globin subassemblies in the .apprx.3600 kDa hexagonal bilayer hemoglobins by electrospray ionization time-of-flight mass spectrometry *J. Mol. Biol.* 2001, *309*, 553-560.
81. Nettleton, E. J.; Tito, P.; Sunde, M.; Bouchard, M.; Dobson, C. M.; Robinson, C. V. Characterization of the oligomeric states of insulin in self-assembly and amyloid fibril formation by mass spectrometry *Biophys. J.* 2000, *79*, 1053-1065.
82. Lee, S.-W.; Beauchamp, J. L. Fourier transform ion cyclotron resonance study of multiply charged aggregates of small singly charged peptides formed by electrospray ionization *J. Am. Soc. Mass Spectrom.* 1999, *10*, 347-351.
83. Thomson, B. A. Declustering and Fragmentation of Protein Ions from an Electrospray Ion Source *J. Am. Soc. Mass Spectrom.* 1997, *8*, 1053-1058.

84. Morozov, V. N.; Morozova, T. Y.; Kallenbach, N. R. Atomic force microscopy of structures produced by electrospraying polymer solutions *Int. J. Mass Spectrom.* 1998, *178*, 143-159.
85. Schmittberger, H.; Lierke Ernst, G. ; Battelle Institute E V: USA, 1989.
86. Xie, W. J.; Cao, C. D.; Lu, Y. J.; Wei, B. Eutectic growth under acoustic levitation conditions *Physical Review E: Statistical, Nonlinear, and Soft Matter Physics* 2002, *66*,
87. Brooks, J. S.; Reavis, J. A.; Medwood, R. A.; Stalcup, T. F.; Meisel, M. W.; Steinberg, E.; Arnowitz, L.; Stover, C. C.; Perenboom, J. A. A. J. New opportunities in science, materials, and biological systems in the low-gravity (magnetic levitation) environment (invited) *J. Appl. Phys.* 2000, *87*, 6194-6199.
88. Cedergren, E.; Nilsson, S.; Santesson, S. ; Chemical Holovoice (SE)
Cedergren, Eila (SE)
Nilsson, Staffan (SE)
Santesson, Sabina (SE), 2002.
89. Nilsson, J.; Laurell, T.; Nilsson, S.; Santesson, S.; Patel, L.; Thurmond, R.; Zivin, R. ; Nilsson, Johan (SE)
Laurell, Thomas (SE)
Nilsson, Staffan (SE)
Santesson, Sabina (SE)
Patel, Lekha (US)
Thurmond, Robin (US)
Zivin, Robert (US)
Ortho McNeil Pharm. Inc. (US), 1999.
90. Santesson, S.; Cedergren-Zeppezauer, E. S.; Johansson, T.; Laurell, T.; Nilsson, J.; Nilsson, S. Screening of nucleation conditions using levitated drops for protein crystallization *Anal. Chem.* 2003, *75*, 1733-1740.
91. Santarsiero, B. D.; Yegian, D. T.; Lee, C. C.; Spraggon, G.; Gu, J.; Scheibe, D.; Uber, D. C.; Cornell, E. W.; Nordmeyer, R. A.; Kolbe, W. F.; Jin, J.; Jones, A. L.; Jaflevic, J. M.; Schultz, P. G.; Stevens, R. C. An approach to rapid protein crystallization using nanodroplets *J. Appl. Cryst.* 2002, *35*, 278-281.
92. Ishikawa, Y.; Komada, S. Development of acoustic and electrostatic levitators for containerless protein crystallization *Fujitsu Sci. Tech. J.* 1993, *29*, 330-338.
93. Chung, S. K.; Trinh, E. H. Applications of hybrid ultrasonic-electrostatic levitation to crystal growth and drop dynamics. *FED (Am. Soc. Mech. Eng.)* 1998, *245*, 18/91-18/97.
94. Chung, S. K.; Trinh, E. H. Containerless protein crystal growth in rotating levitated drops *J. Cryst. Growth* 1998, *194*, 384-397.
95. Chung, S. K.; Trinh, E. H. Applications of hybrid ultrasonic-electrostatic levitation to crystal growth and drop dynamics *FED (American Society of Mechanical Engineers)* 1998, *245*, 18/91-18-97.
96. Rhim, W. K.; Chung, S. K. Containerless protein crystal growth method *J. Cryst. Growth* 1991, *110*, 293-301.
97. Rhim, W.-K.; K.Chung, S.; Barber, D.; Man, K. F.; Gutt, G.; Rulison, A.; Spjut, R. E. An electrostatic levitator for high-temperature containerless materials processing in 1-g *Rev. Sci. Instrum.* 1993, *64*, 2961-2970.
98. Rey, C. A.; Sisler, R.; Merkley, D. R.; Danley, T. J. Acoustic levitation for high-temperature containerless processing in space *Prog. Astronaut. Aeronaut.* 1990, *127(Space Commer.: Platforms Process.)*, 270-285.
99. Bancel, P. A.; Cajipe, V. B.; Rodier, F. Manipulating crystals with light *J. Cryst. Growth* 1999, *196*, 685-690.
100. Myerson, A. S. , 2003.

101. Zaccaro, J.; Matic, J.; Myerson, A. S.; Garetz, B. A. Nonphotochemical, laser-induced nucleation of supersaturated aqueous glycine
produces unexpected g-polymorph *Crystal Growth & Design* 2001, *1*, 5-8.
102. Park, H. K.; Grigoropoulos, C. P.; Yavas, O.; Poon, C. C.; Tam, A. C. Laser-induced nucleation and cavitation at a liquid-solid interface *HTD (American Society of Mechanical Engineers)* 1994, *291*,
103. Binder, K. Is laser-induced nucleation due to a bulk long-wavelength instability? *Journal de Physique, Colloque* 1980, *C4*, 75-78.
104. Wang, W.; Liao, K.; Wang, B.; Xiao, J. In *Proceedings of SPIE-The International Society for Optical Engineering (1999)*, 1999; Vol. 3862(Industrial Lasers (IL '99)), pp 479-483.
105. Gadomski, A.; Siodmiak, J. A novel model of protein crystal growth: Kinetic limits, length scales and the role of the double layer *Croatia Chemica Acta* 2003, *76*, 129-136.
106. Sear, R. P. Protein crystals and charged surfaces: Interactions and heterogeneous nucleation *Phys. Rev. E* 2003, *67*, 061907/1-011907/7.
107. Sear, R. P. Distribution of the second virial coefficients of globular proteins *Europhys. Lett.* 2002, *60*, 938-944.
108. Sear, R. P.; Warren, P. B. On the electrical double layer contribution to the interfacial tension of protein crystals *J. Chem. Phys.* 2002, *117*, 8074-8079.
109. Avassoli, Z.; Sear, R. P. Homogeneous nucleation near a second phase transition and Ostwald's step rule *J. Chem. Phys.* 2002, *116*, 5066-5072.
110. Bechtold, I. H.; De Santo, M. P.; Bonvent, J. J.; Oliveira, E. A.; Barberi, R.; Rasing, T. Rubbing-induced charge domains observed by electrostatic force microscopy: effect on liquid crystal alignment *Liquid Crystals* 2003, *30*, 591-598.
111. Schmitz, K. S. Surface Charge Induced Reentrant Crystalline-Liquid Transition in Colloidal Systems: The Role of the Microion Disposition *Langmuir* 2001, *17*, 8028-8039.
112. Thomas, N. E.; Coakley, W. T. Localized contact formation by erythrocyte membranes: electrostatic effects *Biophys. J.* 1995, *69*, 1387-1401.
113. Coakley, W. T.; Gallez, D.; Thomas, N. E.; Baker, A. J. An interfacial instability approach to erythrocyte adhesion by macromolecules *Colloids Surf., B* 1994, *2*, 281-290.
114. Klotz, S. A. The contribution of electrostatic forces to the process of adherence of Candida albicans yeast cells to substrates *FEMS Microbiol. Lett.* 1994, *120*, 257-262.
115. Bunt, C. R.; Jones, D. S.; Tucker, I. G. The effects of pH, ionic strength and organic phase on the bacterial adhesion to hydrocarbons (BATH) test *Int. J. Pharm.* 1993, *99*, 93-98.
116. Vernhet, A.; Leveau, J. Y.; Cerf, O.; Bellon-Fontaine, M. N. Role of electrostatic interactions in Saccharomyces cerevisiae adhesion to the inner surface of champagne bottles. *Biofouling* 1992, *5*, 323-334.
117. Chang, Y. I. The effect of cationic electrolytes on the electrostatic behavior of cellular surfaces with ionizable groups *J. Theor. Biol.* 1989, *139*, 561-571.
118. Bengtsson, G.; Lindqvist, R.; Piwoni, M. D. Sorption of trace organics to colloidal clays, polymers, and bacteria *Soil Sci. Soc. Am. J.* 1993, *57*, 12961-12970.
119. Clegg, S.; Forster, C. F.; Crabtree, R. W. An examination into the attachment of bio-organic material to the mineral particles in sewer sediments *Environ. Tech.* 1993, *14*, 463-470.
120. Hanczyc, M. M.; Fujikawa, S. M.; Szotstak, J. W. Experimental models of primitive cellular compartments: Encapsulation, growth, and division *Science* 2003, *302*, 618-622.
121. Ertem, G.; Ferris, J. P. Template-directed synthesis using the heterogeneous templates produced by montmorillonite catalysis: A possible bridge between the prebiotic and RNA worlds *J. Am. Chem. Soc.* 1997, *119*, 7197-7201.
122. Ferris, J. P.; Hill, A. R.; Liu, R.; Orgel, L. E. Synthesis of long prebiotic oligomers on mineral surfaces *Nature* 1996, *381*, 59-61.

123. Prakash, J.; Ferris, J. P.; Pitsch, S. Homochiral selection in the montmorillonite-catalyzed and uncatalyzed prebiotic synthesis of RNA *Chem. Comm.* 2000, *24*, 2497-2498.
124. Sowerby, S. J.; Edelwirth, M.; Heckl, W. M. Self-assembly at the prebiotic solid-liquid interface: Structures of self-assembled monolayers of adenine and guanine bases formed on inorganic surfaces *J. Phys. Chem. B* 1998, *102*, 5914-5922.
125. Huber, C.; Wachtershauser, G. Peptides by activation of amino acids with CO on (Ni,Fe)S surfaces: Implications for the origin of life *Science* 1998, *281*, 670-672.
126. Huber, C.; Wachtershauser, G. Activated acetic acid by carbon fixation on (Fe,Ni)S under primordial conditions *Science* 1997, *276*, 245-247.
127. Cody, G. D.; Boctor, N. Z.; Filley, T. R.; Hazen, R. M.; Scott, J. H.; Sharma, A.; Yoder, H. S. Primordial carbonylated iron-sulfur compounds and the synthesis of pyruvate *Science* 2000, *289*, 1337-1340.
128. Smith, J. V.; Arnold, F. P.; Parsons, I.; Lee, M. R. Biochemical evolution III: Polymerization on organophilic silica-rich surfaces, crystal-chemical modeling, formation of first cells, and geological clues *Proc. natl. Acad. Sci. USA* 1999, *96*, 3479-3485.
129. Smith, J. V. Biochemical evolution. I. Polymerization on internal, organophilic silica surfaces of dealuminated zeolites and feldspars *Proc. Natl. Acad. Sci. USA* 1998, *95*, 3370-3375.
130. Williams, R. J. P. The fundamental nature of life as a chemical system: the part played by inorganic elements *J. Inorg. Biochem.* 2002, *88*, 241-250.
131. Bogan, M. J.; Agnes, G. R. Wall-less sample preparation of micrometer-sized sample spots for femtomole detection limits of proteins from liquid based UV-MALDI matrices *submitted to J. Am. Soc. Mass Spectrom., June 25* 2003,
132. Millikan, R. A. *Phys. Rev.* 1909, *30*, 560.
133. Millikan, R. A. *Phys. Rev.* 1913, *2*, 109-143.
134. Paul, W. Electromagnetic Traps for Charged and neutral particles *Reviews of Modern Physics* 1990, *62*, 531-540.
135. Wuerker, R. F.; Shelton, H.; Langmuir, R. V. Electrodynamic containment of charged particles *J. Appl. Phys.* 1959, *30*, 342.
136. Davis, E. J.; Buehler, M. F.; Ward, T. L. The double-ring electrodynamic balance for microparticle characterization *Rev. Sci. Instrum.* 1990, *61*, 1281-1288.
137. Davis, E. J. A History of Single Aerosol Particle Levitation *Aerosol Sci. Technol.* 1997, *26*, 212-254.
138. Feng, X.; Agnes, G. R. Single isolated droplets with net charge as a source of ions *J. Am. Soc. Mass Spectrom.* 2000, *11*, 393-399.
139. Xu, Y.; Bruening, M. L.; Watson, J. T. Non-specific, on-probe cleanup methods for MALDI-MS samples *Mass Spectrom. Rev.* 2003, *22*, 429-440.
140. Luxembourg, S. L.; McDonnell, L. A.; Duursma, M. C.; Guo, X.; Heeren, R. M. A. Effect of local matrix crystal variations in matrix-assisted ionization techniques for mass spectrometry *Anal. Chem.* 2003, *75*, 2333-2341.
141. McDonnell, L. A.; Mize, T. H.; Luxembourg, S. L.; Koster, S.; Eijkel, G. B.; Verpoorte, E.; de Rooij, N. F.; Heeren, R. M. A. Using matrix peaks to map topography: Increased mass resolution and enhanced sensitivity in chemical imaging *Anal. Chem.* 2003, *75*, 4373-4381.